DNA replication during acute MEK inhibition drives acquisition of resistance through amplification of the *BRAF* oncogene

Prasanna Channathodiyil[1,2], Anne Segonds-Pichon[3], Paul D. Smith[4], Simon J. Cook[5] and Jonathan Houseley[1,6,*]

[1] Epigenetics Programme, Babraham Institute, Cambridge, UK
[2] ORCID: 0000-0002-9381-6089
[3] Babraham Bioinformatics, Babraham Institute, Cambridge, UK. ORCID: 0000-0002-8369-4882
[4] Oncology R&D, AstraZeneca CRUK Cambridge Institute, Cambridge, UK
[5] Signalling programme, Babraham Institute, Cambridge, UK. ORCID: 0000-0001-9087-1616
[6] ORCID: 0000-0001-8509-1500
[*] Corresponding author: jon.houseley@babraham.ac.uk

Abstract

Mutations and gene amplifications that confer drug resistance emerge frequently during chemotherapy, but their mechanism and timing is poorly understood. Here, we investigate *BRAF*[V600E] amplification events that underlie resistance to the MEK inhibitor selumetinib (AZD6244/ARRY-142886) in COLO205 cells. We find that de novo focal *BRAF* amplification is the primary path to resistance irrespective of pre-existing amplifications. Although selumetinib causes long-term G1 arrest, we observe that cells stochastically re-enter the cell cycle during treatment without reactivation of ERK1/2 or induction of a normal proliferative gene expression programme. Genes encoding DNA replication and repair factors are downregulated during G1 arrest, but many are transiently induced when cells escape arrest and enter S and G2. Nonetheless, mRNAs encoding key DNA replication factors including the MCM replicative helicase complex, PCNA and TIPIN remain at very low abundance, which likely explains previous reports of replication stress and mutagenesis under long-term RAF-MEK-ERK1/2 pathway inhibition. To test the hypothesis that DNA replication in drug promotes de novo *BRAF* amplification, we exploited the combination of palbociclib and selumetinib to reinforce the G1 arrest. Using a palbociclib dose that suppresses cell cycle entry during selumetinib treatment but not during normal proliferation, we show that combined treatment robustly delays the emergence of drug resistant colonies. Our results demonstrate that acquisition of MEK inhibitor resistance can occur through de novo gene amplification events resulting from DNA replication in drug, and is suppressed by drug combinations that impede cell cycle entry.

Introduction

The development of targeted anti-cancer drugs has improved treatment efficacy and reduced side effects but drug resistance still limits long-term patient survival (*1, 2*). Mutations and gene amplifications affecting the drug target or proteins in downstream pathways allow re-emergence of tumours that are refractory to treatment with the original and related chemotherapeutics (*3, 4*). For example, tumours resistant to the EGFR inhibitors gefitinib and erlotinib normally carry *EGFR^T790M* mutations that impair drug binding, or *MET* amplifications that bypass EGFR to activate PI3K-Akt signalling (*5-7*).

In addition to PI3K, EGFR activates the RAS-RAF-MEK-ERK1/2 pathway (hereafter, ERK1/2 pathway), a major regulator of cell survival and proliferation. Constitutive activation of this pathway resulting from mutational activation of BRAF or RAS proteins occurs in the majority of melanomas and colorectal cancers (*8, 9*). Consequently, the ERK1/2 pathway is a major target for drug development and inhibitors of RAF and MEK are approved for treatment of melanoma, whilst ERK1/2 inhibitors are undergoing clinical trials; however, patients often relapse with drug-resistant tumours (*10, 11*)**.** Selumetinib (AZD6244/ARRY-142886) is a highly specific MEK inhibitor (MEKi) that suppresses constitutive activity of the ERK1/2 pathway, shows promise in pre-clinical studies (*12-14*) and has been approved for paediatric neurofibromatosis type 1 (NF1). However, resistance to MEKi arises frequently through amplification of *BRAF* or *RAS* (*15-19*) or through MEK mutation (*20*).

Cancer cells are genetically heterogeneous and rare pre-existing mutations that confer drug resistance may be selected for during treatment (*21, 22*). However, de novo mutations that occur during drug exposure can also cause resistance (*23*), in which case cells must survive initial drug application and then acquire mutations that restore proliferation. In culture, and recently in vivo, small numbers of drug tolerant persister (DTP) cells have been observed to survive extended treatment with targeted chemotherapeutics (*24-27*). DTPs exist in a non-proliferative or slow cycling state with gene expression patterns and metabolic states distinct from untreated and resistant populations (*24-26, 28-31*). However, proliferative colonies routinely emerge from DTPs in the presence of drug after long periods of apparent stasis, marking the DTP state as a precursor to resistance (*23, 25-27*). DTPs do not stem from a genetically defined subpopulation in the parental cell line and are not inherently drug resistant since removal from drug restores normal susceptibility (*24, 26, 27*); instead DTPs represent an epigenetic state of the parental cell line that is dependent on histone demethylases and deacetylases for maintenance (*25, 27, 28, 30*).

Colonies of resistant cells derived from DTPs carry drug resistance mutations of unknown provenance. For example, erlotinib-resistant clones derived from a single clonal parental cell line exhibited diverse mutations including single nucleotide variants and gene amplifications in components of the ERK1/2 pathway (*32*). These clones formed from a clonal parental cell line with kinetics matching de novo rather than pre-existing erlotinib-resistance mutations (*23, 32*), suggesting that mutations arise de novo during treatment. Recently, EGFR inhibition amongst other treatments was shown to downregulate DNA replication and repair genes

while inducing error prone DNA polymerase genes, which may represent an adaptive mutability response to chemotherapeutic challenge (*33-35*). However, slow cycling cells in unchallenged populations exhibit a similar gene expression signature (*36*), and upregulation of error prone DNA polymerases is not necessarily mutagenic (*37*). Therefore, changes in expression of genome maintenance factors may be a consequence of the transition to a slow-growing DTP state and may not be innately mutagenic.

The cause of de novo mutations in DTPs, whether accidental or actively induced, is of great interest as mutagenic mechanisms that act during therapy could be inhibited to slow the acquisition of resistance. Here, we demonstrate that selumetinib resistance arises predominantly through de novo *BRAF* amplifications in colorectal cancer cells. We further show that DTPs occasionally enter S phase during selumetinib treatment without inducing key cell cycle-regulated DNA replication genes, potentially providing a mutagenic environment for the emergence of de novo gene amplifications. Finally, we show that reducing the frequency with which DTPs replicate delays the emergence of selumetinib resistance.

Results

Selumetinib resistance in COLO205 cells arises primarily through de novo BRAF^{V600E} amplification

Colorectal cancer cells carrying the *BRAF^{V600E}* mutation can overcome MEK inhibition by amplification of *BRAF^{V600E}*, increasing levels of BRAF^{V600E} protein to activate more MEK and sustain ERK1/2 activity (*15, 16*). However, such *BRAF^{V600E}*-amplified cells become addicted to MEKi; withdrawal of MEKi drives excessive MEK-ERK1/2 activity due to amplified BRAF^{V600E}, resulting in cell cycle arrest, senescence and apoptosis (*16, 38*). This in turn suggests that de novo *BRAF* amplifications may be the cause of MEKi resistance because *BRAF^{V600E}* amplifications sufficient for resistance would not be tolerated in a drug-naïve cell. Nonetheless, pre-existing *BRAF*-amplified cells (~4%) have been reported in drug naïve colorectal cancer cells (*15*). These conflicting observations, made in cell lines derived from the same tumour, led us to investigate the contributions of pre-existing and de novo *BRAF^{V600E}* amplifications to the emergence of MEKi resistance.

To determine the frequency of *BRAF^{V600E}* amplification among independently-derived resistant clones, 24 replicate cultures of COLO205 were treated with 1 μM selumetinib (~10 times the IC_{50} value for inhibition of proliferation of the parental cells (*16*)) for 8-10 weeks until proliferating drug-resistant clones were observed in 23/24 cultures (Fig. 1A). As a culture may contain multiple resistant clones, we purified each resistant culture by re-derivation from a single cell maintained in selumetinib. qPCR for *BRAF* copy number revealed a variable but at least 3-fold amplification of *BRAF* in 21 of 23 resistant cell lines (91%), demonstrating that acquisition of selumetinib resistance through *BRAF* amplification is reproducible and frequent in COLO205 cells (Fig. 1B) (*38*). Normalisation of *BRAF* qPCR to control loci on the same chromosome or a different chromosome gave equivalent results, showing that *BRAF* is subject

to focal amplification rather than whole chromosome aneuploidy (compare Fig. S1A to Fig. 1B).

If *BRAF*-amplified cell lines derive from a pre-existing subpopulation, they will show identical amplification breakpoints in multiple independently derived cell lines. To test this, we acquired copy number profiles from parental COLO205 cells and 7 selumetinib-resistant cell lines using CytoSNP-850K Beadchip arrays. All seven resistant cell lines carried focal amplifications in the region encompassing *BRAF* (7q34) (Fig. 1C) whilst few copy number aberrations were detected elsewhere beyond those inherited from the parental cell line (Fig. S1B). Three of these resistant cell lines showed identical and characteristic patterns of amplification in and around the *BRAF* locus that must stem from a pre-existing subpopulation in the parental cell line (Fig. 1C clones e-g). These three cell lines carried an associated amplification at 7q32 (128 Mb in Fig. 1C), and qPCR for the *RBM28* gene at 7q32 in all 23 resistant cell lines detected amplification in these 3 cell lines and an additional 2 not tested by Beadchip array (Fig. S1C), meaning that 5/23 (22%) resistant cell lines likely arose from a single pre-existing population. However, focal amplifications in the other resistant clones had unique breakpoints that could represent de novo amplifications (Fig. 1C clones a-d).

To determine whether selumetinib-resistant clones emerge from diverse pre-existing *BRAF*-amplified subpopulations, we erased existing population heterogeneity by deriving clonal COLO205 cell lines. All ten clonal cell lines were sensitive to 1 μM selumetinib, ceasing proliferation within 1 day of treatment, and all engendered proliferative drug resistant colonies upon prolonged selumetinib treatment. Remarkably, the time required for resistant colonies to appear in nine of the clonal cell lines was identical to parental COLO205 cells, with one clone being slower though not significantly so (Fig. 1D). This shows that pre-existing *BRAF*-amplified cells in the parental COLO205 cell line are not required for and contribute little to the timing of selumetinib resistance. Furthermore, *BRAF* locus structure was different in each of eight resistant cell lines derived independently from 3 clonal COLO205 cell lines (Fig. 1E). Therefore, suppression of existing population heterogeneity does not alter the time required for acquisition of selumetinib resistance and unique de novo *BRAF* amplifications arise frequently (7/8 cell lines). It is also worth noting that one resistant cell line showed no detectable amplification of *BRAF*, meaning that other mutations (or epigenetic changes) conferring resistance also arise de novo (Fig. 1E clone 4-b).

Together, these experiments reveal that amplification of $BRAF^{V600E}$ occurs frequently in COLO205 cells. Although pre-existing amplifications are present, these make a minor contribution to resistance, which emerges efficiently through de novo gene amplification.

Individual cells enter the cell cycle even under acute MEK inhibition

Inactivation of the ERK1/2 pathway by MEK inhibition induces G1 cell cycle arrest in $BRAF^{V600E}$ cell lines including COLO205 (*39, 40*). The treatment conditions used in this study result in growth arrest of COLO205 cells with no passaging required across six or more weeks in the presence of drug; instead, gradual cell death occurs over many weeks with remaining DTPs

aggregating into large bodies from which resistant colonies often, but not always, emerge (Fig. 2A). De novo gene copy number amplifications normally arise through defective DNA replication, breakage-fusion-bridge cycles or extrachromosomal DNA mis-segregation, all of which are prevented by G1 arrest (*41, 42*). We therefore hypothesised that cells occasionally enter the cell cycle even in the presence of selumetinib, and that these cells are at risk of genome instability. Indeed, such events were recently reported during treatment with BRAF and EGFR inhibitors (*31, 43*).

To test this hypothesis, selumetinib-treated COLO205 cells were pulsed with the thymidine analogue ethynyl deoxyuridine (EdU), and labelled cells analysed by flow cytometry and imaging. A 4-hour pulse of EdU plus selumetinib applied after 24 hours pre-treatment with selumetinib alone labelled $4.9 \pm 0.3\%$ of cells, compared to $43 \pm 4\%$ of control cells (Fig 2B), confirming that a fraction of COLO205 cells continue to enter DNA replication in the presence of selumetinib. Such cells are detected at all times analysed up to at least 7 days after selumetinib application (Fig S2A), showing that cells continue to enter replication over prolonged drug treatment. The pre-existing *BRAF*-amplified subpopulation in the parental cell line may continue to replicate in drug, however equivalent assays in clonal COLO205 cell lines, which lack this subpopulation, revealed $4.7 \pm 2\%$ EdU positive cells after 24 hours selumetinib compared to $44 \pm 6\%$ in untreated controls (Fig. 2B), showing that EdU-positive cells do not represent the pre-existing *BRAF* amplified subpopulation. Staining both for EdU incorporation and the G2 marker Cyclin B1 (CCNB1) revealed that ~30% of EdU positive cells are also positive for CCNB1 in both selumetinib treated and untreated populations (Fig. 2C), and DAPI incorporation in EdU/CCNB1 double-positive cells is consistent with 4n genome content (Fig. S2B). These data show that cells can escape the G1 arrest mediated by selumetinib and progress through the cell cycle. To ensure that escape from arrest is not unique to COLO205 cells, we analysed another *BRAF^{V600E}* mutant colorectal cancer cell line, HT29, and observed a similar proportion of EdU positive cells (Fig. S2C). Similarly, we observed replicating cells after treatment of COLO205 cells with the MEKi trametinib, showing that escape from G1 and entry to replication is not unique to selumetinib treatment (Fig. S2D).

Stochastic escape from G1 arrest would explain the presence of EdU-positive cells, but so would a defined subpopulation remaining proliferative in the presence of selumetinib. To distinguish these possibilities, we first treated cells continuously for 11 days with EdU + selumetinib, during which time almost half the cells incorporated EdU (Fig. 2D). We then performed an EdU pulse-chase experiment, treating cells for 1 day with selumetinib alone, 1 day with selumetinib + EdU, then 5 days in selumetinib alone. Almost 10% of cells were EdU-labelled in the initial pulse, but during the 5-day chase this number decreased suggesting that the labelled subpopulation progressively die off rather than proliferate (Fig. 2E, bottom left). Furthermore, the EdU intensity did not decrease showing that EdU positive cells do not divide further (Fig. 2E, bottom right). It is important to note that EdU alone causes this arrest as we see the same effect in the absence of selumetinib (Fig. S2E); nevertheless, if cells arrest on EdU incorporation then the progressive increase in EdU-positive cells across time means that

the population as a whole remains competent to escape G1 arrest and undergo DNA replication.

These results demonstrate that cells stochastically escape selumetinib mediated G1 arrest and progress through S phase to G2. These DNA replication events provide an opportunity for de novo gene amplification, particularly if replication is sub-optimal.

Abnormal gene expression during cell cycle progression in selumetinib

A substantial number of genes involved in DNA replication are regulated indirectly by the ERK1/2 pathway, and suppression of ERK1/2 signalling through EGFR inhibition downregulates DNA repair genes (*35, 44-46*). MEK inhibition could therefore cause impaired and error prone DNA replication if not reversed on entry to S phase, but transient ERK1/2 reactivation may coincide with escape from G1 arrest as reported for BRAF inhibition (*43*). We therefore assayed ERK1/2 activation by high-throughput imaging for ERK1/2 phosphorylated at T202/Y204 (pERK). As expected, a 24-hour treatment with selumetinib dramatically reduced pERK compared to untreated controls, with similar reductions observed in both EdU negative and EdU positive fractions (Fig. 3A). This shows that ERK1/2 are not reactivated in cells that have initiated DNA replication in the presence of selumetinib, and therefore replication may occur with improper gene expression.

Initial RNA-seq analysis across a 48-hour selumetinib treatment revealed vast transcriptomic changes in accord with the known G1 arrest and suppression of growth (Fig. 3B). Transcripts significantly downregulated across the time course segregated into a rapidly responding group enriched in signal transduction genes, particularly the MAPK pathway (*47*), and a slower responding group only substantially depleted 24 hours after selumetinib treatment. The latter group was highly enriched for ribosome biogenesis, cell cycle and DNA repair and replication genes, as expected for a population entering G1 arrest; however, these changes may be reversed on cell cycle re-entry.

To study the rare replicating cells, we developed a method for gene expression analysis after fixation, staining and sorting cells for intracellular markers (*48*). We then applied this method to enrich for CCNB1-positive G2 cells in selumetinib-treated and control populations, obtaining high quality RNA and mRNA-seq libraries (Fig. S3A and S3B). In accord with the pERK imaging data, CCNB1-positive cells in selumetinib did not re-induce genes repressed by MEK inhibition (Fig. S3C) (*47*), nor display the known transcriptomic signature of MEK functional output (Fig. S3D) (*49*). Therefore, even if replication is initiated by transient ERK1/2 activation this has no lasting impact on the transcriptome. We then filtered RNA-seq data for the 1561 transcripts significantly and substantially (>4-fold) differentially expressed between at least two of the four conditions (untreated/selumetinib-treated and CCNB1 -ve/+ve). These transcripts separated into 3 hierarchical clusters: cluster (i) genes are downregulated by selumetinib treatment irrespective of cell cycle stage; cluster (ii) genes are downregulated in selumetinib-treated CCNB1 negative cells but re-expressed in CCNB1 positive cells; cluster (iii) genes are upregulated on selumetinib treatment irrespective of cell cycle (Fig. 3C).

Cluster (i) contains well-characterised ERK1/2 targets including *CCND1* (encoding Cyclin D1), *DUSP4/5/6* and *SPRED1/2*. However, most prominent amongst GO enrichments for this cluster are terms relating to DNA replication, driven by transcripts encoding the entire MCM complex, CDC45, GINS components, replicative polymerase epsilon and alpha subunits, and other important replication proteins including PCNA, FEN1, TIPIN and CLSPN. Many of these genes are transcriptionally activated by E2F transcription factors (*50-52*), and transcripts encoding E2F1 and E2F2 also feature in this cluster as do the E2F targets *CCNE1* and *CCNE2* encoding cyclins E1 and E2. Although the proteins encoded by these transcripts would have already performed their replicative function before accumulation of CCNB1 at G2, the fact that all of these transcripts are dramatically lower in selumetinib-treated G2 cells compared to untreated G2 cells shows that the regulation of these genes is impaired by selumetinib. In contrast, cluster (ii) transcripts are downregulated in the bulk selumetinib-treated population but induce to normal levels in G2 cells. GO analysis of this cluster reveals strong enrichments for mitotic cell cycle and terms associated with chromosome segregation, microtubule organisation and centromeric chromatin deposition. This cluster also includes genes for DNA repair factors involved in processing stalled and damaged replication forks such as *BRCA2, BLM, GEN1* and *POLQ*, showing that chromosome segregation and DNA repair genes can be induced as required in G2 irrespective of ERK1/2 signalling. Cluster (iii) contained genes in a wide range of functional categories and was not significantly enriched for any GO category.

Although this analysis demonstrates that key replication genes are mis-expressed during cells escaping selumetinib-induced G1 arrest, profiling CCNB1-positive cells would miss a transient upregulation of transcripts during S phase. To address this, we optimised a protocol for recovering RNA from sorted EdU-positive cells that provided RNA of sufficient quality for mRNA-seq library construction, although RNA integrity was lower than we would normally use since Click-labelling degrades RNA (Fig. S3E, S3F). Reassuringly, transcript levels in EdU-positive cells from selumetinib-treated and control populations were similar to CCNB1-positive cells across the differentially expressed clusters (Fig. S3F), with expected differences such as *CCNB1* mRNA being 4-fold lower in EdU positive than CCNB1-positive fractions and *CCNE1* and *CCNE2* (unstable mRNAs encoding Cyclin E) being higher. However, a subset of the genes in cluster (i) is upregulated in EdU-positive selumetinib-treated cells compared to CCNB1-positive or negative cells, showing that transient re-expression does occur in S phase (Fig. S3F upper panel, highlighted in orange). This set includes mRNAs for E2F1, E2F2 and key DNA replication proteins including CLSPN, POLE2 and POLA2 (Fig. 3D, upper genes). In contrast, other genes vital for DNA replication fidelity remained repressed in the EdU-positive fraction including the MCM complex, FEN1, TIPIN and PCNA. Notably, deficiencies in any one of these have been shown to cause genome instability (*53-57*) (Figure 3D, lower genes).

Together, these data show that in the presence of selumetinib, a fraction of cells can enter S phase without reactivation of ERK1/2 signalling. Although many cell cycle-regulated genes are induced to normal levels as cells enter the cell cycle, a subset of genes encoding key

replication factors remain downregulated throughout the cell cycle. This increases the chance of DNA replication errors that may give rise to de novo genome rearrangements.

Replication during MEK inhibition facilitates the emergence of drug resistance

These changes in gene expression might suggest a rapid shift to a mutagenic state upon selumetinib application, but proteins such as MCMs and PCNA are long-lived and so levels only decline slowly (*58-60*). We applied high-throughput imaging to quantify MCM2 and MCM7 in EdU-negative and positive cells over 1-week and 3-week time-courses (Fig. 4A and S4A), and observed that levels of both proteins decreased over the first week in the EdU-negative (G1) population as predicted, then remained stable for the following 2 weeks. Prior to selumetinib treatment, levels of MCM2 and MCM7 were similar in EdU-negative (G1) and EdU-positive (S and G2) cells (Fig. 4A, untreated), but entry to S phase in the presence of selumetinib must involve synthesis of MCM proteins as MCM2 and MCM7 were substantially more abundant in EdU-positive than EdU-negative cells (Fig. 4A, 1-3 weeks). This may nonetheless be insufficient to maintain normal DNA replication as MCM7 is still less abundant under selumetinib than in normal S phase (Fig. 4A left panel, note that in EdU-positive cells, the median MCM7 level for each of the selumetinib-treated time points lies in the bottom quartile of MCM7 levels in untreated cells). Furthermore MCM2 is expressed to a higher level than in untreated cells meaning that the abundance of the stoichiometric MCM complex members is unbalanced (Fig. 4A right panel, note that for EdU-positive cells, the median MCM2 level for each of the selumetinib-treated time points lies in the top quartile of MCM2 levels in untreated cells).

These changes in protein level are subtle, but sub-optimal MCM protein levels and imbalances are known to cause genome instability and sensitivity to replication stress (*55, 56, 61, 62*), raising the hypothesis that DNA replication during long-term drug treatment would carry a higher frequency of de novo DNA rearrangements, including gene amplifications such as we observe at *BRAF*. It follows that if the frequency with which cells enter DNA replication during drug treatment can be reduced then the formation of selumetinib resistant clones that result from de novo gene amplification events should be retarded.

Reduced *CCND1* expression caused by selumetinib treatment (Fig. S4B) must decrease the activity of CCND1-CDK4/6, reducing Rb phosphorylation and impairing cell cycle entry (*63, 64*). Recent studies have shown that MEKi can combine well with CDK4/6i in melanoma to further suppress proliferation (*65, 66*) so we examined this combination in our colorectal cancer model. Indeed the combination of selumetinib with a low dose of the CDK4/6i palbociclib further reduced the already low levels of phosphorylated Rb (pRb) (Fig. 4B). In contrast, this dose of palbociclib had no discernible effect on pRb in the absence of selumetinib, nor was the total level of Rb altered by palbociclib in the presence or absence of selumetinib (Fig. 4B). EdU incorporation assays confirmed that this dose of palbociclib had no impact on entry to the cell cycle in the absence of selumetinib but further reduced the fraction of EdU positive cells in the presence of selumetinib 10-fold (Fig. 4C, 4D). Furthermore, this concentration of palbociclib had no effect on cell proliferation or colony formation by parental

COLO205 cells in the absence of selumetinib (Fig. S4C, S4D). Therefore, palbociclib acts in combination with selumetinib to decrease the population of replicating cells.

We then compared the time taken for proliferating drug-resistant colonies to emerge in cultures treated with selumetinib alone or with a combination of selumetinib and low dose palbociclib in the parental COLO205 cell line and 4 single cell-derived clones. Resistant colonies formed in 86% of cultures, and average *BRAF* amplifications were equivalent for resistant cell lines derived under both conditions showing that palbociclib does not prevent acquisition of resistance through *BRAF* amplification (Fig. S4E). Curiously, although all tested resistant cell lines derived on selumetinib alone carried *BRAF* amplifications, a subset of those derived on the combination did not, suggesting alternative paths to resistance become important (Fig. S4D). However, the addition of palbociclib slowed the emergence of resistant clones substantially and significantly in all 5 cell lines, delaying the median time to resistance (where measurable) by three to eight weeks (Fig. 4E, 4F). We used a Cox Proportional-Hazards Model to quantify the overall effect of low dose palbociclib in combination with selumetinib compared to selumetinib alone, and found that palbociclib reduced the risk of resistance by 78% with $p=1.6 \times 10^{-11}$. Differences between the COLO205 cell lines had no significant effect on palbociclib action (p=0.93), even though there was a significant difference between the cell lines in acquisition of resistance in general ($p=1.1 \times 10^{-10}$). For example, clone 1 was slow to obtain resistance here as in Fig. 1D ($p=5.5 \times 10^6$) but took even longer to develop resistance under combined treatment with palbociclib.

Taken together, our experiments show that in most cases selumetinib resistance in COLO205 cells does not arise from cells with pre-existing amplifications; rather, the majority of gene amplifications causing resistance arise de novo through DNA replication, most likely due to the progressive loss of key replication factors caused by inhibition of ERK1/2 signalling.

Discussion

Here using BRAF[V600E]-mutant colorectal cancer cells addicted to ERK1/2 signalling we show that de novo *BRAF* amplifications arise in selumetinib-treated populations with remarkable efficiency. Cells under continuous selumetinib exposure stochastically escape G1 arrest and enter S phase but do so without inducing a subset of replication factors critical for error-free DNA replication. Escape from G1 arrest is vulnerable to otherwise inert doses of CDK4/6i such that a MEKi+CDK4/6i combination suppresses DNA replication during selumetinib treatment, which retards the emergence of resistance and links de novo gene amplification to DNA replication in drug.

Acquisition of resistance through replication in the presence of drug

The sporadic entry of cells into S phase during drug-imposed G1 arrest has been reported in various cell culture systems (*31, 43*), and downregulation of high fidelity replication and repair

genes has been observed in drug-arrested G1 populations (*33, 35*), suggesting that DNA replication could invoke a general increase in mutability. Here we examined gene expression changes in cells treated with MEKi that escape G1 and progress to S and G2, the cell cycle phases in which DNA replication and high-fidelity DNA repair factors are active. Our analysis of bulk populations treated with selumetinib support previous observations, but we find that many genes important for homologous recombination and repair of defective replication intermediates are re-induced to normal levels in S and G2, likely compensating for any deficit in the G1-arrested population. Similarly, selumetinib-treated cells in G2 show normal expression of genes involved in chromosome segregation. This suggests that even during MEKi treatment, the main mechanisms ensuring faithful transmission of genetic material are normal irrespective of gene expression in the G1-arrested population.

However, a subset of genes encoding critical replication factors remain substantially under-expressed throughout the cell cycle in MEKi-treated cells. The disconnect between mRNA and protein levels is well recognised (*67*), but sustained downregulation of mRNAs encoding critical cell cycle proteins in cells arrested in G1 for days or weeks must reduce resting protein levels, an effect we clearly observe for MCM2 and MCM7. Although additional protein is synthesised in the cells that enter S phase, this does not result in normal balanced protein levels, and may occur too late to offset the deficiency in resting MCM protein levels as MCM complexes need to be loaded during G1 or even the preceding M-phase (*68, 69*). Disruption of MCM complex gene expression is mutagenic in itself (*55, 56, 61, 62*), but the effects on protein level are subtle, and we consider that replication in MEKi-treated cells would be impaired through the sum of small defects in expression of many replication proteins, rather than through MCM proteins alone. This would undermine the fidelity of ongoing DNA replication in drug, providing the conditions for de novo resistance mutations.

Mutability under stress is well characterised in bacteria and has been repeatedly observed in yeast (*70-73*). However, it is hard to prove that such events result from defined programmes that have emerged through selective evolution, against the null hypothesis that mutagenesis is an emergent property of normal maintenance and proliferation systems becoming compromised under stress. We would therefore hesitate to label genome instability caused by under-expression of replication proteins as a mutagenic response, though our study provides strong support for the suggestion that non-genotoxic drug treatment can increase mutation rate and drive the de novo emergence of resistance. Whether mutagenesis is intentional or not, our study and others addressing drug-induced mutation provide grounds for optimism that resistance to targeted chemotherapeutics is preventable, since mutational mechanisms that act during chemotherapy can be characterised and suppressed.

de novo gene amplification promotes reproducible emergence of resistance

Acquiring the correct *BRAF*^V600E copy number presents a challenge: low *BRAF*^V600E copy numbers do not provide sufficient ERK1/2 activity for growth but excessive BRAF^V600E leads to

senescence or apoptosis (*38*). Therefore, the *BRAF* copy number window for proliferation at a given MEKi dose is narrow and, given that pre-existing drug resistant cells are by definition rare, it is unlikely that one or more cells with the required *BRAF* copy number would always exist in a cell population prior to treatment. In contrast, stochastic de novo gene amplification events can eventually encompass all possible copy numbers, such that one or more cells in the population will always acquire the optimal *BRAF* copy number allowing maximum proliferation. This means that de novo acquisition of resistance is much more robust than resistance arising through random pre-existing mutations.

One puzzling feature of drug tolerant persister (DTP) cells that survive for long periods in the presence of chemotherapeutics such as selumetinib is the sharp transition between drug tolerance and proliferation. The bulk population does not slowly re-acquire the ability to proliferate in drug; instead individual colonies of rapidly dividing cells suddenly appear after weeks or months of apparent stasis, requiring a marked return to proliferation in a very small number of cells (*24-27*). The mechanism we propose explains this property; occasional cell division events would not be noticeable in long-term drug treated cultures as these are offset by ongoing cell death. However, if each replication event carries a risk of de novo gene amplification then each cell has a chance of acquiring the correct amplification to allow proliferation during a sporadic replication event. Gene amplifications arising in this manner would manifest as a sudden return of a single cell to proliferation, with an average time-to-resistance defined by the frequency of DNA replication events in drug and the extent to which drug treatment reduces the fidelity of replication.

Indeed, reducing the frequency of replication events with a low dose of palbociclib delayed the formation of resistant clones. Palbociclib was designed as an inhibitor of the CCND1-CDK4/6 complex (*74*), and a simple explanation of this effect would be that low dose palbociclib is sufficient to inhibit residual CCND1-CDK4 complex present after MEKi. However, biochemical analysis shows that palbociclib does not inhibit the active p27-CCND1-CDK4 complex but rather binds to the CDK4 monomer and prevents assembly of p27-CCND1-CDK4 (*75*). In doing so, palbociclib not only prevents CCND1-CDK4 activity but also increases the free pool p27, which inhibits CDK2 (*76, 77*). Therefore, the MEKi + palbociclib combination is complex and may act through both MEKi reducing expression of CCND1 to prevent assembly of active CCND1-CDK4 complexes and palbociclib causing a more complete inhibition of all CDK4 by preventing assembly of all possible CDK4/6-containing complexes, thereby releasing p27 to inhibit CDK2. In any case, the MEKi + palbociclib combination is extremely effective in preventing sporadic entry to S phase, and delays the emergence of de novo proliferative clones carrying *BRAF* amplifications.

Overall, our study shows that pathways to de novo mutation can be mechanistically defined, and present vulnerabilities that can be specifically targeted to slow or stop the acquisition of drug resistance.

Materials and Methods

Cell culture and drug treatment

COLO205 and HT29 colorectal cancer cell lines were provided by the laboratory of Dr. Simon J Cook at the Babraham Institute. Cells were cultured in RPMI-1640 (COLO205) or McCoy's 5A (HT29) media supplemented with 10% (v/v) foetal bovine serum, penicillin (100 U/mL), streptomycin (100 mg/mL) and 2 mM glutamine at 37 °C in a humidified incubator with 5% (v/v) CO_2. Media and reagents were purchased from ThermoFisher Scientific, UK. Cells were routinely tested for mycoplasma contamination using the MycoAlert[TM] Mycoplasma Detection Kit (Lonza, LT07-418). To derive COLO205 cells resistant to selumetinib or to combined treatment with selumetinib and palbociclib (Selleckchem, S111614), cells were seeded in $25cm^2$ cell culture flasks ($1x10^6$ cells per flask) or 6-well plates ($0.5x10^6$ cells per well) in growth media and treated 24 hours later with the concentrations of drugs indicated in the figure legends. Media and drug were changed weekly until colonies ($\geq$50 cells) of proliferating cells were formed in culture.

Cell line identity was validated based on RNA-seq data generated in this work using Cell Line Sleuth, developed by Simon Andrews of the Babraham Institute Bioinformatics Facility (https://github.com/s-andrews/celllinesleuth)

Single cell sorting

To generate single-cell derivatives of parental or selumetinib (1 µM) -resistant (C6244-R) COLO205 cell lines, cells were harvested by trypsinisation, centrifuged (300 x *g* for 5 minutes) and the cell pellet resuspended in fresh media or media containing selumetinib (1 µM) respectively at a cell density of $5x10^6$ cells/ mL. Cells were filtered by passage through a sterile, CellTrics 30 µm filter (Sysmex, 04-004-2326) into 5 mL polypropylene round bottom tubes (Scientific laboratory supplies, 352063) to remove cell clumps and incubated with 1 µg/mL 4, 6-diamidino-2-phenylindole (DAPI) (Sigma, D9542) to allow exclusion of dead cells. DAPI-negative cells were then sorted into 96-well plates containing 100 µL fresh media (parental cells) or media containing selumetinib (1 µM) (selumetinib resistant cells) using a 100 µm nozzle on a BD FACSAria III sorter (BD Biosciences, UK).

EdU staining and immunofluorescence for imaging

Cells were seeded on glass coverslips in 6-well plates and treated 24 hours later with 1 µM Selumetinib followed by addition of 2 or 10 µM EdU as described in the figure legends. Cells were washed once in PBS, fixed with 4% formaldehyde in PBS for 10 minutes, and permeabilised with 0.5% Triton X-100 in PBS for 30 minutes at room temperature (RT). Cells were then washed in 3% BSA and EdU incorporation detected by incubation in click reaction cocktail (43 µL Component D, 387 µL water, 20 µL $CuSO_4$, 50 µL reaction buffer additive (43 µL 10x reaction buffer additive + 387 µL water) and 1.2 µL Alexa Fluor dye) (Click-iT™ EdU

Alexa Fluor™ 594 imaging kit, Thermo Fisher Scientific, C10339) for 30 minutes at RT in dark. The reaction cocktail was removed and cells washed in 3% BSA in PBS and mounted in Vectashield antifade mounting medium with DAPI (Vector laboratories, H1200).

For combined detection of EdU incorporation and pERK, MCM2 and MCM7 levels by high-throughput imaging, 1×10^4 cells were seeded per well in 96-well imaging plates (Cell carrier-96, Perkin Elmer) and treated 24 hours later with 1 µM Selumetinib for the duration indicated in the figure legends before addition of 10 µM EdU for 4 hours. Cells were fixed in 4% formaldehyde in PBS, washed with PBS and permeabilised with 100% methanol for 10 minutes at -20 °C. Cells were then washed twice in PBS and EdU labelled using a Click-iT™ EdU Alexa Fluor™ 647 HCS assay kit (Thermo Fisher Scientific, C10357) following manufacturer's instructions. For antibody labelling, cells were incubated in blocking solution (5% normal goat serum and 2% BSA in PBS) for 1 hour at RT, followed by incubation with antibodies against pERK, MCM2 or MCM7 diluted 1:400, 1:400 and 1:200 respectively in 1% BSA and 0.3% Triton X-100 in PBS at 4°C overnight. Antibody diluent without primary antibody was added to background control wells. Cells were washed 3 times in PBS and incubated with secondary antibody (Alexa Fluor 488 donkey anti-rabbit antibody, Thermo Fisher Scientific, A21206) diluted 1:1000 in 1% BSA and 0.3% Triton X-100 in PBS for 1 hour at RT in dark. Cells were washed 3 times in PBS and incubated in 1 µg/mL DAPI (Sigma, D9542) in PBS for 10 minutes at RT. Cells were washed twice in PBS and 100 µL PBS added to each well for imaging. Cells were imaged using an INCell Analyser 6000 Microscope using a 10x objective lens imaging 6 fields (for pERK) or 9 fields (for MCM2 and MCM7) per well. Details of antibodies are provided in Table S4.

Immunolabelling and EdU staining for flow cytometry

Quantitative detection of EdU incorporation was performed using a Click-iT™ EdU Alexa Fluor™ 488 Flow cytometry kit (Thermo Fisher Scientific, C10420) following the manufacturer's instructions. Briefly, cells were incubated with 2 or 10 µM EdU for the time indicated in figure legends. Cells were trypsinised, collected by centrifugation (300 x *g* for 5 minutes at RT) and washed once in PBS. Cells were fixed with Click-iT® fixative for 15 minutes at RT and washed in excess 1% BSA in PBS. Cells were permeabilised in 100 µL 1x saponin-based permeabilisation and wash reagent for 15 minutes or ice-cold 100% methanol (for combined antibody labelling and EdU staining) while vortexing gently for 30 minutes followed by incubation in 250 µL click reaction mix (219 µL PBS, 5 µL CuSO₄, 25 µL 1x buffer additive, 1.25 µL Alexa Fluor dye) for 30 minutes at RT in dark. Cells were washed in excess 1x saponin-based permeabilisation and wash reagent (300 x *g* for 5 minutes). For antibody labelling, cells were blocked for 30 minutes in 1% BSA in PBS, followed by incubation for 1 hour at RT with primary antibody diluted in 1% BSA in PBS. Cells were then washed in PBS and incubated with secondary antibody for 1 hour at RT in dark, after which they were washed again in PBS. Cells were then processed for DNA staining in 1 µg/mL DAPI diluted in 100 µL 1x saponin-based permeabilisation and wash reagent. Cells were filtered to remove aggregates by passage through sterile, 30 µm CellTRics filter (Sysmex, 04-004-2326) into 5 mL polystyrene round-

bottom tubes. Samples were analysed on a Fortessa (BD Biosciences, UK) flow cytometer with a minimum of 10,000 events acquired per sample.

To isolate cells by flow cytometry following EdU or CCNB1 staining, COLO205 cells were seeded at a density of 1×10^6 cells in 25cm^2 cell culture flasks and treated 24 hours later with DMSO or 1 µM selumetinib and/or with 10 µM EdU as indicated in the figure legends. Cells were then processed for immunofluorescence and flow sorting as previously described (*48*). Briefly, cells were harvested by trypsinisation, washed once with PBS and fixed in 3% glyoxal solution (2.8 ml water, 0.79 ml 100% ethanol, 0.31 ml 40% glyoxal (Sigma, 50649) and 30 µl acetic acid; pH adjusted to 4-5 with a few drops of 1M NaOH) and 1:25 RNasin Plus (Promega, N261B) for 15 minutes on ice. Cells were washed in PBS with 1:100 RNasin Plus by centrifugation at 2000 x *g* for 3 minutes at 4°C. Cell pellet was resuspended in 100 µL ice-cold methanol (100% v/v) with 1:25 RNasin Plus (added drop by drop while gently vortexing cells), incubated on ice for 30 minutes and again washed in PBS with 1:100 RNasin Plus by centrifugation at 2000 x *g* for 3 minutes at 4°C. For EdU staining, cells were incubated in a modified click reaction cocktail (209 µL PBS, 5 µL $CuSO_4$, 25 µL 1 M L-ascorbic acid (Sigma, A2174), 1.25 µL Alexa Fluor dye, 10 µL RNasin Plus) Click-iT™ EdU Alexa Fluor™ 488 Flow cytometry kit (Thermo Fisher Scientific, C10420) and incubated on ice for 30 minutes in dark. Following incubation, cells were washed in 1% BSA in PBS and 1:100 RNasin Plus before they were processed for DNA staining. For CCNB1 staining, cells were incubated with primary antibody against CCNB1 (diluted 1:200 in 1% BSA in PBS and 1:25 RNasin Plus) for 1 hour on ice. Cells were washed in PBS with 1:100 RNasin Plus and incubated in fluorescent tagged secondary antibody (diluted 1:1000 in 1% BSA in PBS with 1:25 RNasin Plus) for 30 minutes on ice in dark. Cells were washed again in 1% BSA in PBS with 1:100 RNasin Plus and cell pellet resuspended in 200 µL 1% BSA in PBS with 1:100 RNasin Plus. For DNA staining, cells were incubated in 1 µg/mL DAPI in PBS. Cells were sorted using a 100 µm nozzle on a BD FACSAria III sorter (BD Biosciences, UK) into 1.5ml Eppendorf tubes coated with RNasin plus.

RNA extraction and mRNA-seq library preparation

Cells grown in monolayers were trypsinised, collected by centrifugation (300 x *g* for 5 minutes) and washed once in PBS. Cells sorted by flow cytometry were pelleted by centrifugation (2000 x *g* for 3 minutes). Cells were lysed in 1 mL TRI reagent Sigma, T9424) until a homogeneous lysate was obtained and allowed to stand for 10 minutes at RT. For RNA isolation from cells sorted by flow cytometry, 1 mL TRI reagent was added to cells after they were pelleted by centrifugation (2000 x *g* for 3 minutes at 4°C). The lysate was centrifuged at 12000 x *g* for 15 minutes at 4 °C and the upper aqueous phase containing RNA was collected in fresh tubes to which 0.5 mL 2-propanol was added, mixed well and allowed to stand for 10 minutes. For RNA extraction from <50,000 cells, 1 µL GlycoBlue coprecipitant 15 mg/mL (ThermoFisher scientific, AM9516) was added to the mixture to aid the visibility of RNA pellets. The resulting mixture was centrifuged (12,000 × g for 10 minutes at 4 °C) and supernatant discarded. RNA pellets were washed in 1 mL 75% (v/v) ethanol by centrifugation

at 7,500 x *g* for 5 minutes at 4 °C. Pellets were then air-dried for 5-10 minutes and resuspended in 10-20 µL nuclease-free water.

RNA integrity was assessed by electrophoresis on a denaturing agarose gel and/or a Bioanalyzer 6000 pico chip (Agilent 5067-1513). mRNA seq libraries were prepared using the NEBNext ultra (NEB E7420S) (or ultra II) Directional RNA kit (NEB E7760S) with the NEBNext Poly(A) mRNA Magnetic Isolation Module (NEB E7490S), following the protocol provided by the manufacturer with the exception that two successive 0.9x AMPure purifications were performed on the final amplified libraries. Libraries were amplified for 12-14 cycles. Library quality was assessed on a Bioanalyzer 2100 using High Sensitivity DNA chips (Agilent 5067-4626) and quantification performed with a KAPA Library Quantification Kit (Roche, KK4844). Libraries were sequenced by the Babraham Institute Next Generation Sequencing Facility on an Illumina HiSeq2500 in Rapid Run 50bp Single End mode.

mRNA-seq data analysis

After adapter and quality trimming using Trim Galore (v0.5.0), RNAseq data was mapped to human genome GRCh38 using HISAT2 v2.1.0 (*78*) by the Babraham Institute Bioinformatics Facility. Mapped data was imported into SeqMonk v1.47.0 (https://www.bioinformatics.babraham.ac.uk/projects/seqmonk/) and normalised to total read count. DESeq2 analyses (*79*) was performed within SeqMonk using a p-value cut-off of 0.01, and significantly different genes were further filtered for genes with >4-fold difference in at least one comparison. Hierarchical clustering analysis was performed using SeqMonk, and GO analysis of individual clusters performed using GOrilla (http://cbl-gorilla.cs.technion.ac.il/) (*80, 81*). Quoted p-values for GO analysis are FDR-corrected according to the Benjamini and Hochberg method (q-values from the GOrilla output), for brevity only the order of magnitude rather than the full q-value is given (*82*).

All sequencing data is available through GEO accession: GSE168604.

DNA extraction and qPCR

Genomic DNA from cells was extracted using a Qiagen DNeasy Blood and Tissue kit (Qiagen, 69504), according to the manufacturer's instructions. DNA (2 µg) was digested with a restriction enzyme that does not cut the amplicons (*Eco*RI, NEB R3101) by incubation at 37°C for 1 hour. The digested products were purified using a QIAquick PCR purification kit (Qiagen, 28106) according to the manufacturer's instructions. For each qPCR reaction, 4 µL purified DNA (1 µg/µL) was mixed with 5 µL 2x Maxima SYBR mix, 0.2 µl each of forward and reverse primers (10 µM) and 0.6 µl nuclease-free water. The PCR cycling conditions were initial denaturation at 95°C for 10 minutes, followed by 40 cycles of denaturation at 95°C for 15 seconds and extension at 60°C for 1 min on the Bio-Rad CFX qPCR machine (Bio-Rad, UK). Data were analysed with CFX manager software v.3.1. Details of primer sequences are provided in Table S5.

CNV microarray

Total DNA from cells was isolated using a Qiagen DNeasy Blood and Tissue kit (Qiagen, 69504) and DNA quality was assessed using a Nanodrop 2000 Spectrophotometer (ThermoFisher Scientific, UK) to determine A260/A280 and A260/A230 ratios, and by electrophoresis on 1% agarose gel to confirm absence of degradation. DNA quantity was estimated using a Quant-iT PicoGreen dsDNA assay kit (ThermoFisher Scientific, P7589) following instructions provided by the manufacturer. DNA samples (200 ng per sample) were processed by Cambridge genomics services (Department of Pathology, Cambridge) for hybridisation onto cytoSNP 850K beadchips (Illumina) according to the manufacturer's instructions. The raw intensity data files (.idat) were converted to genotype call files (.gtc) using Beeline software version 4.5 then imported to BlueFuse Multi software version 4.5 and analysed using BlueFuse algorithm with default settings (10 contiguous markers for CNV and 500 contiguous markers for loss of heterozygosity (LOH)). The cluster and manifest files used for processing Illumina CytoSNP-850K v1.1 were CytoSNP-850Kv1-1_iScan_C1_ClusterFile.egt and CytoSNP-850Kv1-1_iScan_C1.bpm respectively and CytoSNP-850Kv1-2_iScan_B1_ClusterFile.egt and CytoSNP-850Kv1-2_iScan_B3.bpm respectively for Illumina CytoSNP-850K v1.2 beadchips. The annotation file used for the analysis was BG_Annotation_Ens74_20180801.db (genome build 37).

All array data is available through GEO accession: GSE168604.

Protein extraction and Western blot

Preparation of cell lysates for SDS-PAGE and western blotting were performed as previously described (*38*). Cells grown in 25cm^2 cell culture flasks were detached using a cell scrapper, centrifuged (300 x *g* for 3 minutes), washed once with PBS and lysed for 5 minutes with ice-cold TG lysis buffer (20 mM Tris-HCl (pH 7.4), 137 mM NaCl, 1 mM EGTA, 1% (v/v) Triton X-100, 10% (v/v) glycerol, 1.5 mM MgCl$_2$, 50 mM NaF, 1 mM Na$_3$VO$_4$, 5 µg mL^{-1} aprotinin, 10 µg mL^{-1} leupeptin, 1 mM phenylmethylsulfonyl fluoride (PMSF). Cell lysates were centrifuged for 10 minutes at 13,000 x *g* at 4 °C. Protein concentration was estimated by Bradford protein assay and absorbance read at 562 nm using a Pherastar plate reader (BMG labtech, UK). Protein samples were boiled for 5 minutes in 4x sample buffer (50 mM Tris-HCl (pH 6.8), 2% (w/v) SDS, 10% (v/v) glycerol, 1% (v/v) β-mercaptoethanol, 0.01% (w/v) bromophenol blue).

Total protein was subjected to electrophoresis through a 10% SDS-PAGE gel for 4 hours at 75 V, transferred to methanol-activated Immobilon-FL polyvinylidene difluoride (PVDF) membranes (Merck Millipore, Watford, UK) by wet transfer (0.2 M glycine, 25 mM Tris, 20% (v/v) methanol) at 20 V overnight. Membranes were blocked with a blocking buffer (5% milk in Tris buffered saline and Tween 20 (TBST) (5% (w/v) non-fat powdered milk, 10 mM Tris-HCl (pH 7.6), 150 mM NaCl, 0.1% (v/v) Tween-20) for 1 hour at room temperature. Membranes were incubated with primary antibodies against CCND1, p27, phospho RB, RB and GAPDH as recommended in 5% milk in TBST or 5% BSA in TBST overnight at 4°C with gentle agitation, after which they were washed in TBST (3x 10 minute washes) and incubated with fluorescent tagged secondary antibodies (diluted 1:30,000 in 5% milk in TBST) for 1 hour at room

temperature in dark. Membranes were again washed (3 x 10 minute washes) before detection of bands using a Li-Cor Odyssey Imaging System (LI-COR Biosciences). Details of antibodies are provided in Table S4.

Colony formation assay

COLO205 cells (0.25×10^6 cells/well) were seeded in 6-well plates and treated with 16 nM palbociclib or DMSO only 24 hours later. Following 24 hours of treatment, cells were harvested by trypsinisation, counted by a Countess cell counter (ThermoFisher Scientific) and 100 cells seeded per well in 6-well plates in culture media each in the absence or presence of 16 nM palbociclib in triplicates. Cells were incubated for 21 days, with media and drug replenished once a week. To stain colonies, cells were gently washed once in PBS and fixed and stained with crystal violet (0.4% (w/v), Sigma, C6158) in 50% methanol for at least 30 minutes. Excess stain was carefully removed from cells by gently immersing the culture plate several times in a trough filled with cold tap water. Plates were air-dried at room temperature.

Statistical analysis

Statistical tests were performed using GraphPad Prism v8.4.0, except the Cox Proportional-Hazards Model, which was implemented in RStudio v1.2.5033. Code is available on GitHub https://github.com/segondsa/resistant-colonies

Conflict of interest statement
PDS is a paid employee and shareholder of AstraZeneca plc. The remaining authors declare no conflicts of interest.

References

1. L. A. Garraway, P. A. Janne, Circumventing cancer drug resistance in the era of personalized medicine. *Cancer Discov* **2**, 214-226 (2012).
2. N. Vasan, J. Baselga, D. M. Hyman, A view on drug resistance in cancer. *Nature* **575**, 299-309 (2019).
3. C. M. Lovly, A. T. Shaw, Molecular pathways: resistance to kinase inhibitors and implications for therapeutic strategies. *Clin Cancer Res* **20**, 2249-2256 (2014).
4. A. A. Samatar, P. I. Poulikakos, Targeting RAS-ERK signalling in cancer: promises and challenges. *Nat Rev Drug Discov* **13**, 928-942 (2014).
5. M. N. Balak, Y. Gong, G. J. Riely, R. Somwar, A. R. Li, M. F. Zakowski, A. Chiang, G. Yang, O. Ouerfelli, M. G. Kris, M. Ladanyi, V. A. Miller, W. Pao, Novel D761Y and common secondary T790M mutations in epidermal growth factor receptor-mutant lung adenocarcinomas with acquired resistance to kinase inhibitors. *Clin Cancer Res* **12**, 6494-6501 (2006).
6. J. A. Engelman, K. Zejnullahu, T. Mitsudomi, Y. Song, C. Hyland, J. O. Park, N. Lindeman, C. M. Gale, X. Zhao, J. Christensen, T. Kosaka, A. J. Holmes, A. M. Rogers, F. Cappuzzo, T. Mok, C. Lee, B. E. Johnson, L. C. Cantley, P. A. Janne, MET amplification leads to gefitinib resistance in lung cancer by activating ERBB3 signaling. *Science* **316**, 1039-1043 (2007).
7. T. Kosaka, Y. Yatabe, H. Endoh, K. Yoshida, T. Hida, M. Tsuboi, H. Tada, H. Kuwano, T. Mitsudomi, Analysis of epidermal growth factor receptor gene mutation in patients with non-small cell lung cancer and acquired resistance to gefitinib. *Clin Cancer Res* **12**, 5764-5769 (2006).
8. H. Davies, G. R. Bignell, C. Cox, P. Stephens, S. Edkins, S. Clegg, J. Teague, H. Woffendin, M. J. Garnett, W. Bottomley, N. Davis, E. Dicks, R. Ewing, Y. Floyd, K. Gray, S. Hall, R. Hawes, J. Hughes, V. Kosmidou, A. Menzies, C. Mould, A. Parker, C. Stevens, S. Watt, S. Hooper, R. Wilson, H. Jayatilake, B. A. Gusterson, C. Cooper, J. Shipley, D. Hargrave, K. Pritchard-Jones, N. Maitland, G. Chenevix-Trench, G. J. Riggins, D. D. Bigner, G. Palmieri, A. Cossu, A. Flanagan, A. Nicholson, J. W. Ho, S. Y. Leung, S. T. Yuen, B. L. Weber, H. F. Seigler, T. L. Darrow, H. Paterson, R. Marais, C. J. Marshall, R. Wooster, M. R. Stratton, P. A. Futreal, Mutations of the BRAF gene in human cancer. *Nature* **417**, 949-954 (2002).
9. R. Yaeger, R. B. Corcoran, Targeting Alterations in the RAF-MEK Pathway. *Cancer Discov* **9**, 329-341 (2019).
10. C. J. Caunt, M. J. Sale, P. D. Smith, S. J. Cook, MEK1 and MEK2 inhibitors and cancer therapy: the long and winding road. *Nat Rev Cancer* **15**, 577-592 (2015).
11. M. Holderfield, M. M. Deuker, F. McCormick, M. McMahon, Targeting RAF kinases for cancer therapy: BRAF-mutated melanoma and beyond. *Nat Rev Cancer* **14**, 455-467 (2014).
12. K. K. Ciombor, T. Bekaii-Saab, Selumetinib for the treatment of cancer. *Expert Opin Investig Drugs* **24**, 111-123 (2015).
13. B. R. Davies, A. Logie, J. S. McKay, P. Martin, S. Steele, R. Jenkins, M. Cockerill, S. Cartlidge, P. D. Smith, AZD6244 (ARRY-142886), a potent inhibitor of mitogen-activated protein kinase/extracellular signal-regulated kinase kinase 1/2 kinases: mechanism of action in vivo, pharmacokinetic/pharmacodynamic relationship, and potential for combination in preclinical models. *Mol Cancer Ther* **6**, 2209-2219 (2007).
14. T. C. Yeh, V. Marsh, B. A. Bernat, J. Ballard, H. Colwell, R. J. Evans, J. Parry, D. Smith, B. J. Brandhuber, S. Gross, A. Marlow, B. Hurley, J. Lyssikatos, P. A. Lee, J. D. Winkler, K. Koch, E. Wallace, Biological characterization of ARRY-142886 (AZD6244), a potent, highly selective mitogen-activated protein kinase kinase 1/2 inhibitor. *Clin Cancer Res* **13**, 1576-1583 (2007).
15. R. B. Corcoran, D. Dias-Santagata, K. Bergethon, A. J. Iafrate, J. Settleman, J. A. Engelman, BRAF gene amplification can promote acquired resistance to MEK inhibitors in cancer cells harboring the BRAF V600E mutation. *Sci Signal* **3**, ra84 (2010).

16.   A. S. Little, K. Balmanno, M. J. Sale, S. Newman, J. R. Dry, M. Hampson, P. A. Edwards, P. D. Smith, S. J. Cook, Amplification of the driving oncogene, KRAS or BRAF, underpins acquired resistance to MEK1/2 inhibitors in colorectal cancer cells. *Sci Signal* **4**, ra17 (2011).

17.   G. V. Long, C. Fung, A. M. Menzies, G. M. Pupo, M. S. Carlino, J. Hyman, H. Shahheydari, V. Tembe, J. F. Thompson, R. P. Saw, J. Howle, N. K. Hayward, P. Johansson, R. A. Scolyer, R. F. Kefford, H. Rizos, Increased MAPK reactivation in early resistance to dabrafenib/trametinib combination therapy of BRAF-mutant metastatic melanoma. *Nat Commun* **5**, 5694 (2014).

18.   D. Oddo, E. M. Sennott, L. Barault, E. Valtorta, S. Arena, A. Cassingena, G. Filiciotto, G. Marzolla, E. Elez, R. M. van Geel, A. Bartolini, G. Crisafulli, V. Boscaro, J. T. Godfrey, M. Buscarino, C. Cancelliere, M. Linnebacher, G. Corti, M. Truini, G. Siravegna, J. Grasselli, M. Gallicchio, R. Bernards, J. H. Schellens, J. Tabernero, J. A. Engelman, A. Sartore-Bianchi, A. Bardelli, S. Siena, R. B. Corcoran, F. Di Nicolantonio, Molecular Landscape of Acquired Resistance to Targeted Therapy Combinations in BRAF-Mutant Colorectal Cancer. *Cancer Res* **76**, 4504-4515 (2016).

19.   H. Shi, G. Moriceau, X. Kong, M. K. Lee, H. Lee, R. C. Koya, C. Ng, T. Chodon, R. A. Scolyer, K. B. Dahlman, J. A. Sosman, R. F. Kefford, G. V. Long, S. F. Nelson, A. Ribas, R. S. Lo, Melanoma whole-exome sequencing identifies (V600E)B-RAF amplification-mediated acquired B-RAF inhibitor resistance. *Nat Commun* **3**, 724 (2012).

20.   C. M. Emery, K. G. Vijayendran, M. C. Zipser, A. M. Sawyer, L. Niu, J. J. Kim, C. Hatton, R. Chopra, P. A. Oberholzer, M. B. Karpova, L. E. MacConaill, J. Zhang, N. S. Gray, W. R. Sellers, R. Dummer, L. A. Garraway, MEK1 mutations confer resistance to MEK and B-RAF inhibition. *Proc Natl Acad Sci U S A* **106**, 20411-20416 (2009).

21.   H. E. Bhang, D. A. Ruddy, V. Krishnamurthy Radhakrishna, J. X. Caushi, R. Zhao, M. M. Hims, A. P. Singh, I. Kao, D. Rakiec, P. Shaw, M. Balak, A. Raza, E. Ackley, N. Keen, M. R. Schlabach, M. Palmer, R. J. Leary, D. Y. Chiang, W. R. Sellers, F. Michor, V. G. Cooke, J. M. Korn, F. Stegmeier, Studying clonal dynamics in response to cancer therapy using high-complexity barcoding. *Nat Med* **21**, 440-448 (2015).

22.   L. A. Diaz, Jr., R. T. Williams, J. Wu, I. Kinde, J. R. Hecht, J. Berlin, B. Allen, I. Bozic, J. G. Reiter, M. A. Nowak, K. W. Kinzler, K. S. Oliner, B. Vogelstein, The molecular evolution of acquired resistance to targeted EGFR blockade in colorectal cancers. *Nature* **486**, 537-540 (2012).

23.   A. N. Hata, M. J. Niederst, H. L. Archibald, M. Gomez-Caraballo, F. M. Siddiqui, H. E. Mulvey, Y. E. Maruvka, F. Ji, H. E. Bhang, V. Krishnamurthy Radhakrishna, G. Siravegna, H. Hu, S. Raoof, E. Lockerman, A. Kalsy, D. Lee, C. L. Keating, D. A. Ruddy, L. J. Damon, A. S. Crystal, C. Costa, Z. Piotrowska, A. Bardelli, A. J. Iafrate, R. I. Sadreyev, F. Stegmeier, G. Getz, L. V. Sequist, A. C. Faber, J. A. Engelman, Tumor cells can follow distinct evolutionary paths to become resistant to epidermal growth factor receptor inhibition. *Nat Med* **22**, 262-269 (2016).

24.   G. V. Echeverria, Z. Ge, S. Seth, X. Zhang, S. Jeter-Jones, X. Zhou, S. Cai, Y. Tu, A. McCoy, M. Peoples, Y. Sun, H. Qiu, Q. Chang, C. Bristow, A. Carugo, J. Shao, X. Ma, A. Harris, P. Mundi, R. Lau, V. Ramamoorthy, Y. Wu, M. J. Alvarez, A. Califano, S. L. Moulder, W. F. Symmans, J. R. Marszalek, T. P. Heffernan, J. T. Chang, H. Piwnica-Worms, Resistance to neoadjuvant chemotherapy in triple-negative breast cancer mediated by a reversible drug-tolerant state. *Sci Transl Med* **11**, (2019).

25.   D. Ravindran Menon, S. Das, C. Krepler, A. Vultur, B. Rinner, S. Schauer, K. Kashofer, K. Wagner, G. Zhang, E. Bonyadi Rad, N. K. Haass, H. P. Soyer, B. Gabrielli, R. Somasundaram, G. Hoefler, M. Herlyn, H. Schaider, A stress-induced early innate response causes multidrug tolerance in melanoma. *Oncogene* **34**, 4448-4459 (2015).

26.   S. K. Rehman, J. Haynes, E. Collignon, K. R. Brown, Y. Wang, A. M. L. Nixon, J. P. Bruce, J. A. Wintersinger, A. Singh Mer, E. B. L. Lo, C. Leung, E. Lima-Fernandes, N. M. Pedley, F. Soares, S. McGibbon, H. H. He, A. Pollet, T. J. Pugh, B. Haibe-Kains, Q. Morris, M. Ramalho-Santos, S. Goyal, J. Moffat, C. A. O'Brien, Colorectal Cancer Cells Enter a Diapause-like DTP State to Survive Chemotherapy. *Cell* **184**, 226-242 e221 (2021).

27.   S. V. Sharma, D. Y. Lee, B. Li, M. P. Quinlan, F. Takahashi, S. Maheswaran, U. McDermott, N. Azizian, L. Zou, M. A. Fischbach, K. K. Wong, K. Brandstetter, B. Wittner, S. Ramaswamy, M. Classon, J. Settleman, A chromatin-mediated reversible drug-tolerant state in cancer cell subpopulations. *Cell* **141**, 69-80 (2010).

28.   G. D. Guler, C. A. Tindell, R. Pitti, C. Wilson, K. Nichols, T. KaiWai Cheung, H. J. Kim, M. Wongchenko, Y. Yan, B. Haley, T. Cuellar, J. Webster, N. Alag, G. Hegde, E. Jackson, T. L. Nance, P. G. Giresi, K. B. Chen, J. Liu, S. Jhunjhunwala, J. Settleman, J. P. Stephan, D. Arnott, M. Classon, Repression of Stress-Induced LINE-1 Expression Protects Cancer Cell Subpopulations from Lethal Drug Exposure. *Cancer Cell* **32**, 221-237 e213 (2017).

29.   M. J. Hangauer, V. S. Viswanathan, M. J. Ryan, D. Bole, J. K. Eaton, A. Matov, J. Galeas, H. D. Dhruv, M. E. Berens, S. L. Schreiber, F. McCormick, M. T. McManus, Drug-tolerant persister cancer cells are vulnerable to GPX4 inhibition. *Nature* **551**, 247-250 (2017).

30.   B. B. Liau, C. Sievers, L. K. Donohue, S. M. Gillespie, W. A. Flavahan, T. E. Miller, A. S. Venteicher, C. H. Hebert, C. D. Carey, S. J. Rodig, S. J. Shareef, F. J. Najm, P. van Galen, H. Wakimoto, D. P. Cahill, J. N. Rich, J. C. Aster, M. L. Suva, A. P. Patel, B. E. Bernstein, Adaptive Chromatin Remodeling Drives Glioblastoma Stem Cell Plasticity and Drug Tolerance. *Cell Stem Cell* **20**, 233-246 e237 (2017).

31.   Y. Oren, M. Tsabar, H. F. Cabanos, M. S. Cuoco, E. Zaganjor, P. I. Thakore, M. Tabaka, C. P. Fulco, S. A. Hurvitz, D. J. Slamon, G. Lahav, A. Hata, J. S. Brugge, A. Regev, Cycling cancer persister cells arise from lineages with distinct transcriptional and metabolic programs. *bioRxiv*, 2020.2006.2005.136358 (2020).

32.   M. Ramirez, S. Rajaram, R. J. Steininger, D. Osipchuk, M. A. Roth, L. S. Morinishi, L. Evans, W. Ji, C. H. Hsu, K. Thurley, S. Wei, A. Zhou, P. R. Koduru, B. A. Posner, L. F. Wu, S. J. Altschuler, Diverse drug-resistance mechanisms can emerge from drug-tolerant cancer persister cells. *Nat Commun* **7**, 10690 (2016).

33.   A. Cipponi, D. L. Goode, J. Bedo, M. J. McCabe, M. Pajic, D. R. Croucher, A. G. Rajal, S. R. Junankar, D. N. Saunders, P. Lobachevsky, A. T. Papenfuss, D. Nessem, M. Nobis, S. C. Warren, P. Timpson, M. Cowley, A. C. Vargas, M. R. Qiu, D. G. Generali, S. Keerthikumar, U. Nguyen, N. M. Corcoran, G. V. Long, J. Y. Blay, D. M. Thomas, MTOR signaling orchestrates stress-induced mutagenesis, facilitating adaptive evolution in cancer. *Science* **368**, 1127-1131 (2020).

34.   D. M. Fitzgerald, P. J. Hastings, S. M. Rosenberg, Stress-Induced Mutagenesis: Implications in Cancer and Drug Resistance. *Annu Rev Cancer Biol* **1**, 119-140 (2017).

35.   M. Russo, G. Crisafulli, A. Sogari, N. M. Reilly, S. Arena, S. Lamba, A. Bartolini, V. Amodio, A. Magri, L. Novara, I. Sarotto, Z. D. Nagel, C. G. Piett, A. Amatu, A. Sartore-Bianchi, S. Siena, A. Bertotti, L. Trusolino, M. Corigliano, M. Gherardi, M. C. Lagomarsino, F. Di Nicolantonio, A. Bardelli, Adaptive mutability of colorectal cancers in response to targeted therapies. *Science* **366**, 1473-1480 (2019).

36.   M. Min, S. L. Spencer, Spontaneously slow-cycling subpopulations of human cells originate from activation of stress-response pathways. *PLoS Biol* **17**, e3000178 (2019).

37.   K. Temprine, N. R. Campbell, R. Huang, E. M. Langdon, T. Simon-Vermot, K. Mehta, A. Clapp, M. Chipman, R. M. White, Regulation of the error-prone DNA polymerase Polkappa by oncogenic signaling and its contribution to drug resistance. *Sci Signal* **13**, (2020).

38.   M. J. Sale, K. Balmanno, J. Saxena, E. Ozono, K. Wojdyla, R. E. McIntyre, R. Gilley, A. Woroniuk, K. D. Howarth, G. Hughes, J. R. Dry, M. J. Arends, P. Caro, D. Oxley, S. Ashton, D. J. Adams, J. Saez-Rodriguez, P. D. Smith, S. J. Cook, MEK1/2 inhibitor withdrawal reverses acquired resistance driven by BRAF(V600E) amplification whereas KRAS(G13D) amplification promotes EMT-chemoresistance. *Nat Commun* **10**, 2030 (2019).

39.   M. Cheng, V. Sexl, C. J. Sherr, M. F. Roussel, Assembly of cyclin D-dependent kinase and titration of p27Kip1 regulated by mitogen-activated protein kinase kinase (MEK1). *Proc Natl Acad Sci U S A* **95**, 1091-1096 (1998).

40.   D. B. Solit, L. A. Garraway, C. A. Pratilas, A. Sawai, G. Getz, A. Basso, Q. Ye, J. M. Lobo, Y. She, I. Osman, T. R. Golub, J. Sebolt-Leopold, W. R. Sellers, N. Rosen, BRAF mutation predicts sensitivity to MEK inhibition. *Nature* **439**, 358-362 (2006).

41.   C. Bailey, M. J. Shoura, P. S. Mischel, C. Swanton, Extrachromosomal DNA-relieving heredity constraints, accelerating tumour evolution. *Ann Oncol* **31**, 884-893 (2020).

42.   P. J. Hastings, J. R. Lupski, S. M. Rosenberg, G. Ira, Mechanisms of change in gene copy number. *Nat Rev Genet* **10**, 551-564 (2009).

43.   L. Gerosa, C. Chidley, F. Frohlich, G. Sanchez, S. K. Lim, J. Muhlich, J. Y. Chen, S. Vallabhaneni, G. J. Baker, D. Schapiro, M. I. Atanasova, L. A. Chylek, T. Shi, L. Yi, C. D. Nicora, A. Claas, T. S. C. Ng, R. H. Kohler, D. A. Lauffenburger, R. Weissleder, M. A. Miller, W. J. Qian, H. S. Wiley, P. K. Sorger, Receptor-Driven ERK Pulses Reconfigure MAPK Signaling and Enable Persistence of Drug-Adapted BRAF-Mutant Melanoma Cells. *Cell Syst* **11**, 478-494 e479 (2020).

44.   J. C. Chambard, R. Lefloch, J. Pouyssegur, P. Lenormand, ERK implication in cell cycle regulation. *Biochim Biophys Acta* **1773**, 1299-1310 (2007).

45.   O. Maertens, R. Kuzmickas, H. E. Manchester, C. E. Emerson, A. G. Gavin, C. J. Guild, T. C. Wong, T. De Raedt, C. Bowman-Colin, E. Hatchi, L. A. Garraway, K. T. Flaherty, S. Pathania, S. J. Elledge, K. Cichowski, MAPK Pathway Suppression Unmasks Latent DNA Repair Defects and Confers a Chemical Synthetic Vulnerability in BRAF-, NRAS-, and NF1-Mutant Melanomas. *Cancer Discov* **9**, 526-545 (2019).

46.   F. Vena, R. Jia, A. Esfandiari, J. J. Garcia-Gomez, M. Rodriguez-Justo, J. Ma, S. Syed, L. Crowley, B. Elenbaas, S. Goodstal, J. A. Hartley, D. Hochhauser, MEK inhibition leads to BRCA2 downregulation and sensitization to DNA damaging agents in pancreas and ovarian cancer models. *Oncotarget* **9**, 11592-11603 (2018).

47.   C. A. Pratilas, B. S. Taylor, Q. Ye, A. Viale, C. Sander, D. B. Solit, N. Rosen, (V600E)BRAF is associated with disabled feedback inhibition of RAF-MEK signaling and elevated transcriptional output of the pathway. *Proc Natl Acad Sci U S A* **106**, 4519-4524 (2009).

48.   P. Channathodiyil, J. Houseley, Glyoxal fixation facilitates transcriptome analysis after antigen staining and cell sorting by flow cytometry. *PLoS One* **16**, e0240769 (2021).

49.   J. R. Dry, S. Pavey, C. A. Pratilas, C. Harbron, S. Runswick, D. Hodgson, C. Chresta, R. McCormack, N. Byrne, M. Cockerill, A. Graham, G. Beran, A. Cassidy, C. Haggerty, H. Brown, G. Ellison, J. Dering, B. S. Taylor, M. Stark, V. Bonazzi, S. Ravishankar, L. Packer, F. Xing, D. B. Solit, R. S. Finn, N. Rosen, N. K. Hayward, T. French, P. D. Smith, Transcriptional pathway signatures predict MEK addiction and response to selumetinib (AZD6244). *Cancer Res* **70**, 2264-2273 (2010).

50.   S. Ishida, E. Huang, H. Zuzan, R. Spang, G. Leone, M. West, J. R. Nevins, Role for E2F in control of both DNA replication and mitotic functions as revealed from DNA microarray analysis. *Mol Cell Biol* **21**, 4684-4699 (2001).

51.   R. Iwanaga, H. Komori, S. Ishida, N. Okamura, K. Nakayama, K. I. Nakayama, K. Ohtani, Identification of novel E2F1 target genes regulated in cell cycle-dependent and independent manners. *Oncogene* **25**, 1786-1798 (2006).

52.   K. Ohtani, R. Iwanaga, M. Nakamura, M. Ikeda, N. Yabuta, H. Tsuruga, H. Nojima, Cell growth-regulated expression of mammalian MCM5 and MCM6 genes mediated by the transcription factor E2F. *Oncogene* **18**, 2299-2309 (1999).

53.   E. L. Baple, H. Chambers, H. E. Cross, H. Fawcett, Y. Nakazawa, B. A. Chioza, G. V. Harlalka, S. Mansour, A. Sreekantan-Nair, M. A. Patton, M. Muggenthaler, P. Rich, K. Wagner, R. Coblentz, C. K. Stein, J. I. Last, A. M. Taylor, A. P. Jackson, T. Ogi, A. R. Lehmann, C. M. Green, A. H. Crosby, Hypomorphic PCNA mutation underlies a human DNA repair disorder. *J Clin Invest* **124**, 3137-3146 (2014).

54.   D. M. Chou, S. J. Elledge, Tipin and Timeless form a mutually protective complex required for genotoxic stress resistance and checkpoint function. *Proc Natl Acad Sci U S A* **103**, 18143-18147 (2006).

55.   S. C. Pruitt, K. J. Bailey, A. Freeland, Reduced Mcm2 expression results in severe stem/progenitor cell deficiency and cancer. *Stem Cells* **25**, 3121-3132 (2007).

56.   N. Shima, A. Alcaraz, I. Liachko, T. R. Buske, C. A. Andrews, R. J. Munroe, S. A. Hartford, B. K. Tye, J. C. Schimenti, A viable allele of Mcm4 causes chromosome instability and mammary adenocarcinomas in mice. *Nat Genet* **39**, 93-98 (2007).

57.   L. Zheng, H. Dai, M. Zhou, M. Li, P. Singh, J. Qiu, W. Tsark, Q. Huang, K. Kernstine, X. Zhang, D. Lin, B. Shen, Fen1 mutations result in autoimmunity, chronic inflammation and cancers. *Nat Med* **13**, 812-819 (2007).

58.   R. Bravo, H. Macdonald-Bravo, Existence of two populations of cyclin/proliferating cell nuclear antigen during the cell cycle: association with DNA replication sites. *J Cell Biol* **105**, 1549-1554 (1987).

59.   T. Guida, G. Salvatore, P. Faviana, R. Giannini, G. Garcia-Rostan, L. Provitera, F. Basolo, A. Fusco, F. Carlomagno, M. Santoro, Mitogenic effects of the up-regulation of minichromosome maintenance proteins in anaplastic thyroid carcinoma. *J Clin Endocrinol Metab* **90**, 4703-4709 (2005).

60.   V. Santosa, M. T. Kanemaki, MCMBP maintains genome integrity by protecting the MCM subunits from degradation. *bioRxiv*, 827386 (2019).

61.   C. H. Chuang, M. D. Wallace, C. Abratte, T. Southard, J. C. Schimenti, Incremental genetic perturbations to MCM2-7 expression and subcellular distribution reveal exquisite sensitivity of mice to DNA replication stress. *PLoS Genet* **6**, e1001110 (2010).

62.   X. Q. Ge, D. A. Jackson, J. J. Blow, Dormant origins licensed by excess Mcm2-7 are required for human cells to survive replicative stress. *Genes Dev* **21**, 3331-3341 (2007).

63.   C. Bertoli, J. M. Skotheim, R. A. de Bruin, Control of cell cycle transcription during G1 and S phases. *Nat Rev Mol Cell Biol* **14**, 518-528 (2013).

64.   A. S. Lundberg, R. A. Weinberg, Functional inactivation of the retinoblastoma protein requires sequential modification by at least two distinct cyclin-cdk complexes. *Mol Cell Biol* **18**, 753-761 (1998).

65.   L. N. Kwong, J. C. Costello, H. Liu, S. Jiang, T. L. Helms, A. E. Langsdorf, D. Jakubosky, G. Genovese, F. L. Muller, J. H. Jeong, R. P. Bender, G. C. Chu, K. T. Flaherty, J. A. Wargo, J. J. Collins, L. Chin, Oncogenic NRAS signaling differentially regulates survival and proliferation in melanoma. *Nat Med* **18**, 1503-1510 (2012).

66.   J. A. Sosman, M. Kittaneh, M. P. J. K. Lolkema, M. A. Postow, G. Schwartz, C. Franklin, A. Matano, S. Bhansali, S. Parasuraman, K. Kim, A phase 1b/2 study of LEE011 in combination with binimetinib (MEK162) in patients with NRAS-mutant melanoma: Early encouraging clinical activity. *Journal of Clinical Oncology* **32**, 9009-9009 (2014).

67.   Y. Liu, A. Beyer, R. Aebersold, On the Dependency of Cellular Protein Levels on mRNA Abundance. *Cell* **165**, 535-550 (2016).

68.   D. S. Dimitrova, T. A. Prokhorova, J. J. Blow, I. T. Todorov, D. M. Gilbert, Mammalian nuclei become licensed for DNA replication during late telophase. *J Cell Sci* **115**, 51-59 (2002).

69.   M. A. Kuipers, T. J. Stasevich, T. Sasaki, K. A. Wilson, K. L. Hazelwood, J. G. McNally, M. W. Davidson, D. M. Gilbert, Highly stable loading of Mcm proteins onto chromatin in living cells requires replication to unload. *J Cell Biol* **192**, 29-41 (2011).

70.   G. Chen, W. D. Bradford, C. W. Seidel, R. Li, Hsp90 stress potentiates rapid cellular adaptation through induction of aneuploidy. *Nature* **482**, 246-250 (2012).

71.   B. D. Harrison, J. Hashemi, M. Bibi, R. Pulver, D. Bavli, Y. Nahmias, M. Wellington, G. Sapiro, J. Berman, A tetraploid intermediate precedes aneuploid formation in yeasts exposed to fluconazole. *PLoS Biol* **12**, e1001815 (2014).

72.   S. M. Rosenberg, C. Shee, R. L. Frisch, P. J. Hastings, Stress-induced mutation via DNA breaks in Escherichia coli: a molecular mechanism with implications for evolution and medicine. *Bioessays* **34**, 885-892 (2012).

73.   E. Shor, C. A. Fox, J. R. Broach, The yeast environmental stress response regulates mutagenesis induced by proteotoxic stress. *PLoS Genet* **9**, e1003680 (2013).

74.   D. W. Fry, P. J. Harvey, P. R. Keller, W. L. Elliott, M. Meade, E. Trachet, M. Albassam, X. Zheng, W. R. Leopold, N. K. Pryer, P. L. Toogood, Specific inhibition of cyclin-dependent kinase 4/6 by PD 0332991 and associated antitumor activity in human tumor xenografts. *Mol Cancer Ther* **3**, 1427-1438 (2004).

75.   K. Z. Guiley, J. W. Stevenson, K. Lou, K. J. Barkovich, V. Kumarasamy, T. U. Wijeratne, K. L. Bunch, S. Tripathi, E. S. Knudsen, A. K. Witkiewicz, K. M. Shokat, S. M. Rubin, p27 allosterically activates cyclin-dependent kinase 4 and antagonizes palbociclib inhibition. *Science* **366**, (2019).

76.   N. P. Pavletich, Mechanisms of cyclin-dependent kinase regulation: structures of Cdks, their cyclin activators, and Cip and INK4 inhibitors. *J Mol Biol* **287**, 821-828 (1999).

77.   K. Polyak, M. H. Lee, H. Erdjument-Bromage, A. Koff, J. M. Roberts, P. Tempst, J. Massague, Cloning of p27Kip1, a cyclin-dependent kinase inhibitor and a potential mediator of extracellular antimitogenic signals. *Cell* **78**, 59-66 (1994).

78.   D. Kim, J. M. Paggi, C. Park, C. Bennett, S. L. Salzberg, Graph-based genome alignment and genotyping with HISAT2 and HISAT-genotype. *Nat Biotechnol* **37**, 907-915 (2019).

79.   M. I. Love, W. Huber, S. Anders, Moderated estimation of fold change and dispersion for RNA-seq data with DESeq2. *Genome Biol* **15**, 550 (2014).

80.   E. Eden, D. Lipson, S. Yogev, Z. Yakhini, Discovering motifs in ranked lists of DNA sequences. *PLoS Comput Biol* **3**, e39 (2007).

81.   E. Eden, R. Navon, I. Steinfeld, D. Lipson, Z. Yakhini, GOrilla: a tool for discovery and visualization of enriched GO terms in ranked gene lists. *BMC Bioinformatics* **10**, 48 (2009).

82.   Y. Benjamini, Y. Hochberg, Controlling the False Discovery Rate: A Practical and Powerful Approach to Multiple Testing. *Journal of the Royal Statistical Society: Series B (Methodological)* **57**, 289-300 (1995).
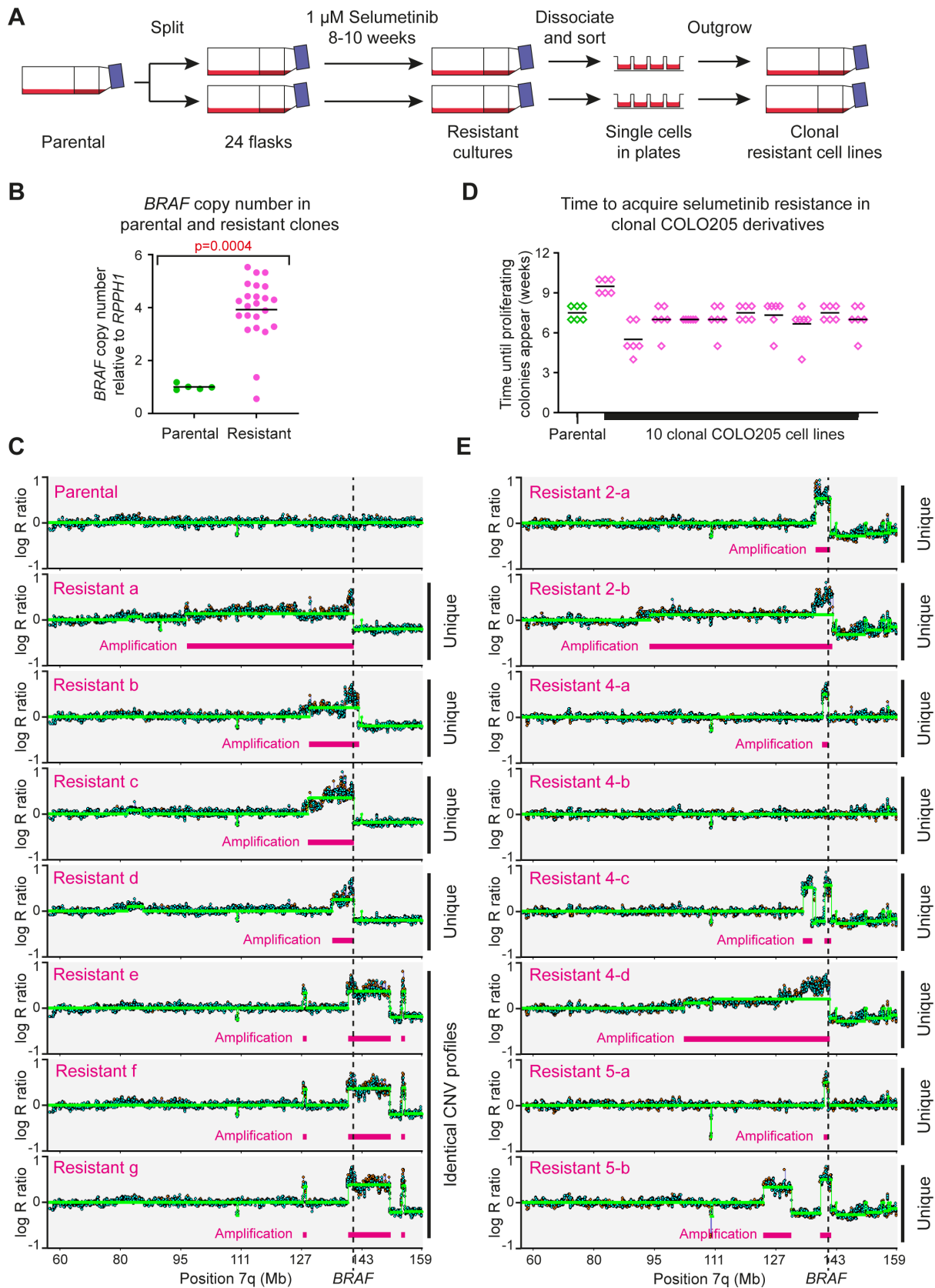
Figures

Figure 1: Contributions of pre-existing and *de novo* gene amplifications to the emergence of selumetinib resistance in COLO205 cells

A: Experimental design for analysing reproducibility of resistance. Proliferating COLO205 cells were seeded in 24 individual 25cm^2 cell culture flasks and 1 µM selumetinib added after 24 hours. Media and drug were changed weekly until colonies of proliferating cells were observed, at which point single cells were isolated by flow cytometry and expanded into separate drug resistant cell lines in the presence of 1 µM selumetinib. After addition of selumetinib, the cell density did not increase and cells were not split across the duration of the treatment.

B: qPCR copy number analysis of *BRAF* relative to *RPPH1* in parental and selumetinib-resistant cell lines derived as in **A**. Data for 5 biological replicates of parental COLO205 cells and 23 independently-derived selumetinib resistant cells lines are shown; 21 of 23 selumetinib resistant cell lines show >3 fold amplification of *BRAF* relative *RPPH1*. Each assay was performed in triplicate. p value was calculated by Mann-Whitney test (n=5 parental, 23 resistant).

C: Copy number profiles of the *BRAF* locus in 7 selumetinib resistant cell lines compared to parental cells, determined using CytoSNP 850K BeadChip arrays (Illumina) and analysed with BlueFuse multi software version 4.5 based on the reference human genome (hg19/GRCh37). Log$_2$ ratio plots of copy number for the q arm of chromosome 7 are shown, including the location of *BRAF* (dotted line) and amplified regions (pink bars). Each resistant cell line derived from clonal amplification of individual selumetinib resistant cells from independent drug treatment flasks, but note that cell lines e, f and g show identical and highly characteristic copy number amplification profiles.

D: Time taken for proliferating selumetinib resistant clones to emerge from parental and 10 different single cell derived COLO205 cell lines. For each cell line, cells were seeded in 6-well plates and treated individually with 1 µM selumetinib after 24 hours. Media and drug were changed weekly, and the time taken until the first colony (≥50 cells) of proliferating cells was observed in each well and recorded (in weeks). The time to resistance was not significantly different between the parental line and any of the clonal lines (p>0.5) by a Kruskal-Wallis test.

E: CNV profiles of the *BRAF* locus in 8 selumetinib resistant lines obtained from clonal parental cell lines, each resistant cell line derived by clonal amplification from an independent drug treatment flask, analysed as in **C**. Three clonal parental cell lines (clonal cell lines 2, 4 and 5) were used, with four resistant clones derived from cell line 4 and 2 each from cell lines 2 and 5. Note that all CNV profiles are different, and that cell line 4-b has become resistant without amplification of the *BRAF* locus or any region detectable by array-based CNV analysis.
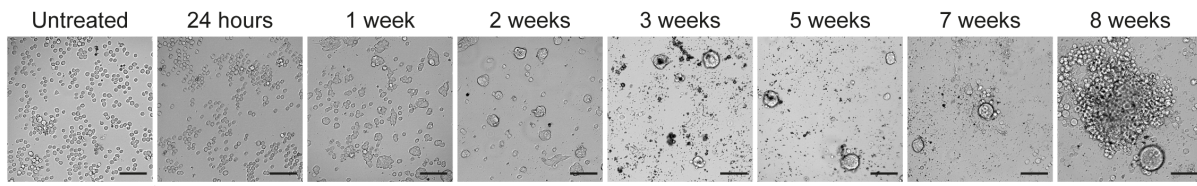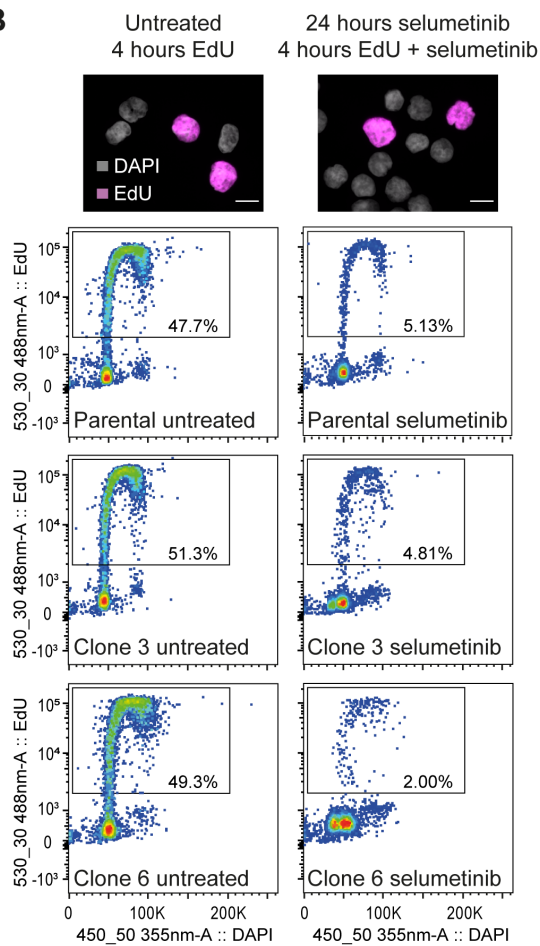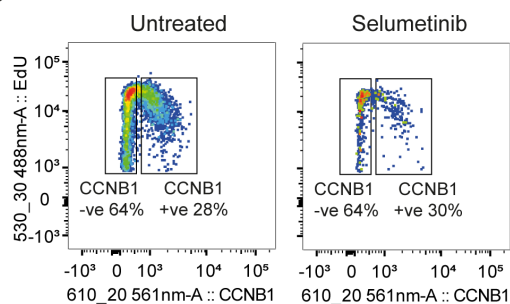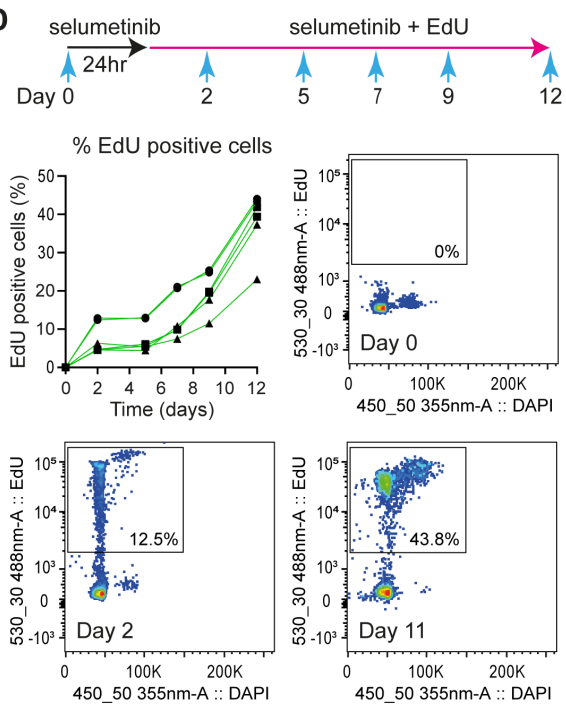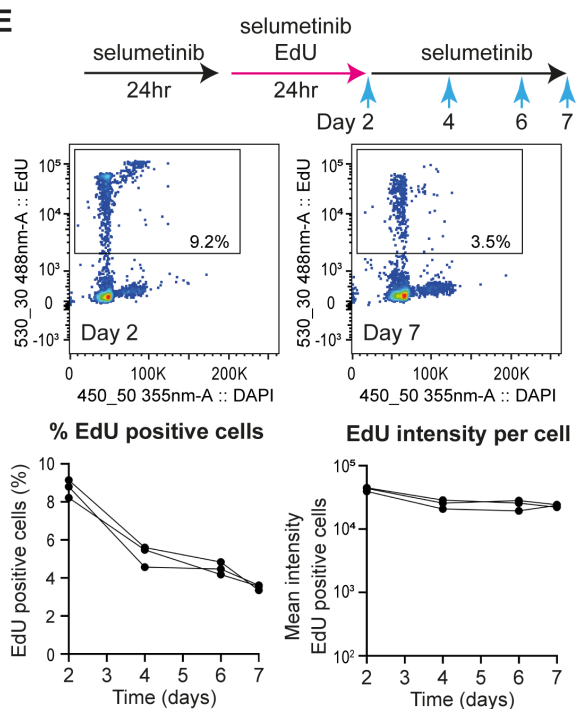
Figure 2: Replicating cells persist in long-term selumetinib-treated cell cultures

A: Representative brightfield images of COLO205 cells during extended treatment with 1 µM selumetinib. Scale bars represent 100 µm.

B: EdU incorporation during selumetinib treatment. COLO205 cells were treated for 24 hours with 1 µM selumetinib before addition of 10 µM EdU for 4 hours. Representative images of EdU negative and positive cells (pink) co-stained with DAPI (grey) from selumetinib treated and control cells are shown at top, scale bars represent 10 µm. Quantification of EdU positive cells in each population by flow cytometry is shown below for parental COLO205 cells and single cell derived clones 3 and 6. Individual plots show EdU incorporation versus DAPI staining of DNA for untreated (left) and selumetinib treated cells (right), with rectangles to indicate gates used to quantify EdU positive and negative cells. Percent EdU positive cells are shown within the gates for each sample.

C: Quantification by flow cytometry of CCNB1 negative and positive cells amongst the EdU positive cell population in untreated (left) and selumetinib treated (right) samples. COLO205 cells were treated with 1 µM selumetinib or DMSO only for 24 hours before addition of 10 µM EdU for 4 hours in the presence or absence of 1 µM selumetinib respectively. Cells were stained with EdU reaction cocktail and counter stained with CCNB1 primary antibody and Alexa Fluor 594 conjugated donkey anti-rabbit secondary antibody. Individual plots show EdU incorporation versus CCNB1 staining for untreated (left) and selumetinib treated (right), with rectangles to indicate gates used to quantify CCNB1 negative and positive cells in the EdU positive population. Percent CCNB1 positive and negative cells are shown within the gates for each sample.

D: Quantification of EdU positive cells by flow cytometry in COLO205 cells grown in the presence of selumetinib and EdU over the course of 11 days. COLO205 cells were treated for 24 hours with 1 µM selumetinib before addition of 2 µM EdU for 6 days, after which cells were rinsed with cell culture media then treated with 1 µM selumetinib and 2 µM EdU for a further 5 days. EdU incorporation was assayed at the indicated time points. Data for 6 independent replicates are shown.

E: EdU positive cells do not increase with prolonged selumetinib treatment. COLO205 cells were treated with 1 µM selumetinib for 24 hours before addition of 2 µM EdU for 24 hours in the presence of 1 µM selumetinib, after which cells were rinsed in cell culture media and grown in the presence of 1 µM selumetinib only for up to 5 days. EdU incorporation was assayed at the indicated time points by flow cytometry. Results are mean of 2 independent replicates. Quantitation of EdU positive cells (left) and EdU intensity per cell (right), n=3 are shown in the bottom panel.

A pERK v. EdU in selumetinib treated and control cells

B Time course of gene expression during first 48 hours of selumetinib treatment

C Genes >4-fold differentially expressed between CCNB1 -ve and +ve in untreated and 24 hour selumetinib-treated cells (1681)
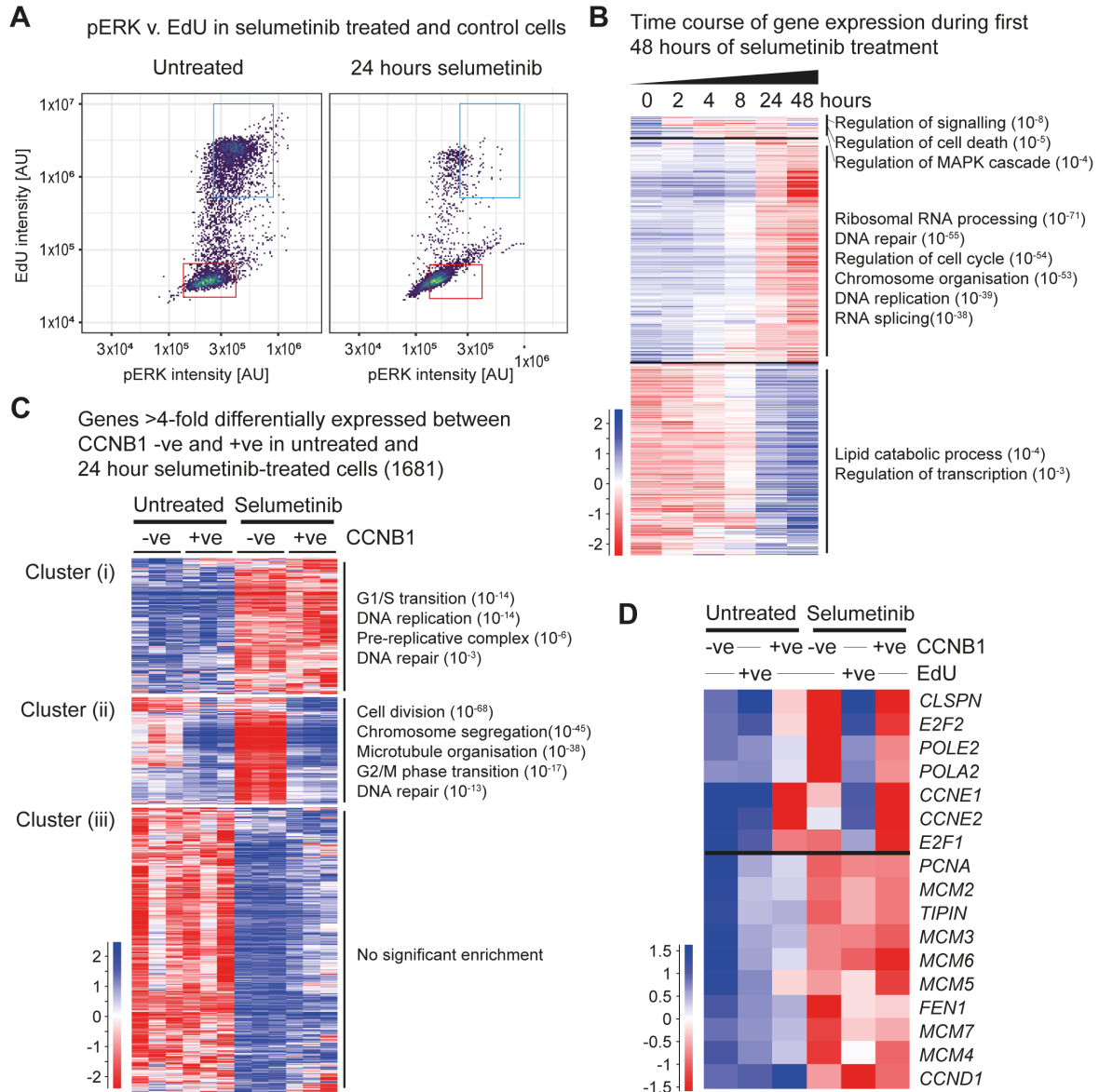
D

Figure 3: COLO205 cells replicating in selumetinib show defective gene expression

A: Quantification of pERK in EdU negative and positive cells. COLO205 cells were treated with 1 μM selumetinib or DMSO only for 24 hours before addition of 10 μM EdU for 4 hours in the presence of 1 μM selumetinib. Following EdU staining and immunofluorescence with pERK (T202/Y204) antibody, EdU incorporation and pERK levels in cells were determined by high content image analysis. EdU and pERK intensity in untreated (left) and selumetinib treated (right) cells normalised to control cells without addition of EdU or pERK primary antibody are shown. EdU negative and positive cells in individual plots are shown in red and blue rectangular gates respectively.

B. Gene expression across time during selumetinib treatment. COLO205 cells were treated with 1 μM selumetinib for up to 48 hours, with cultures harvested at indicated times. The 5782 genes significantly differentially expressed (p<0.05 by DEseq2) between 2 replicates of 0 and 48 hour time points are shown. Genes were categorised into 3 primary behaviours by hierarchical clustering, and representative enriched GO categories (q<0.05) are shown (full GO analysis is presented in Table S1).

C. Differential gene expression between CCNB1 negative and positive COLO205 cells, either untreated or after 24 hours selumetinib treatment. Cells from three biological replicates were fixed with glyoxal, then stained and sorted for CCNB1 followed by mRNAseq library preparation. The 12681 genes shown are significantly (p<0.05 by DEseq2) and substantially (>4-fold) differentially expressed between at least one pair of the four categories shown. Genes were categorised into 3 primary behaviours by hierarchical clustering, and representative enriched GO categories (q<0.05) are shown (full GO analysis is presented in Table S2).

D. Expression of selected replication genes in selumetinib treated and untreated populations sorted for CCNB1 or EdU, representative of the dataset shown in Fig. S3G cluster (i). All genes in this cluster are expressed at a lower level under selumetinib treatment in CCNB1 negative and CCNB1 positive fractions. However the upper cluster of genes is transiently expressed in the S phase population marked by EdU whereas genes in the lower category are not. CCNB1 positive and negative data are an average of 3 datasets.

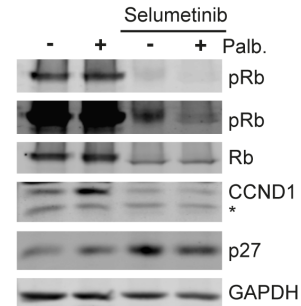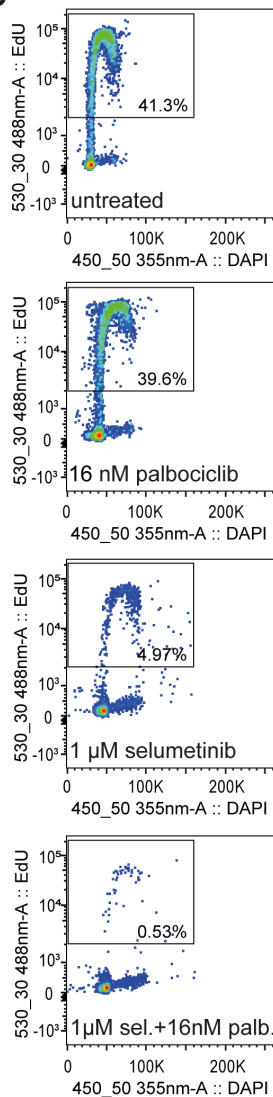**A** MCM2 and MCM7 in EdU -ve and +ve cells during selumetinib treatment
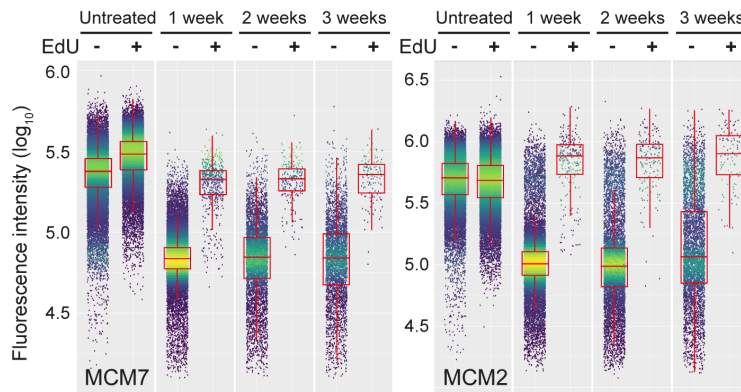
B Effect of selumetinib and palbociclib on pRb

C

D % EdU positive cells

E Time to resistant clone formation

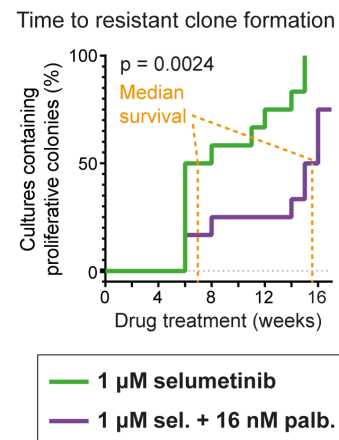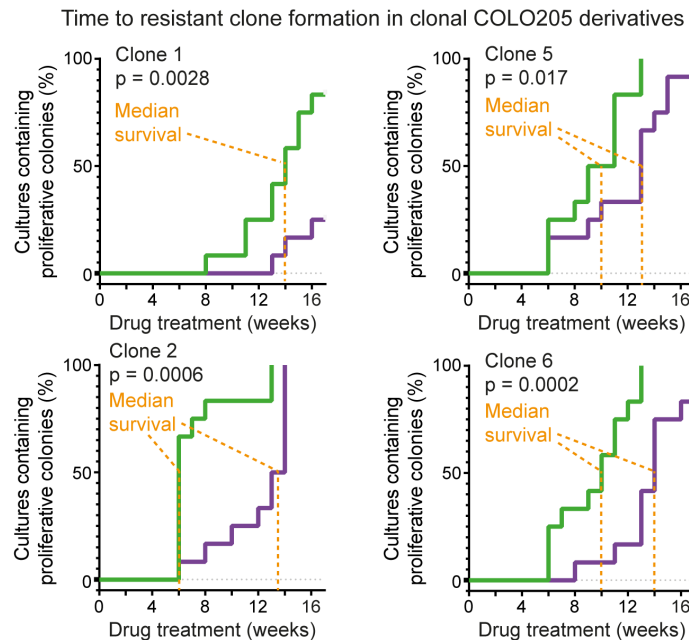**F** Time to resistant clone formation in clonal COLO205 derivatives
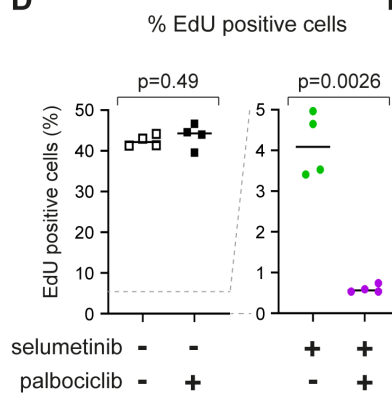
Figure 4: Suppressing DNA replication in selumetinib slows acquisition of resistance

A. Quantification of MCM2 and MCM7 in EdU negative and positive COLO205 cells treated with 1 µM selumetinib or DMSO only (untreated) for 1, 2 and 3 weeks before addition of 10 µM EdU for 4 hours. EdU incorporation and MCM2 and MCM7 levels were determined relative to unstained control cells by high content imaging analysis. Red boxes indicate median signal intensity and inter-quartile range (IQR), whiskers indicate quartile range 1 – 1.5x IQR and quartile range 3 + 1.5x IQR.

B. Western blot analysis of COLO205 cells treated with 1µM selumetinib in the presence (+) or absence (-) of 16 nM palbociclib for 24 hours and with the indicated antibodies. Cells treated with DMSO only or 16 nM palbociclib were included as controls. The pRB panels are shown at two different intensities to make the reduction of pRB levels in the combined selumetinib and palbociclib condition visible. Other panels show total Rb, CCND1, p27 (which is also part of the active CCND1-CDK4/6 complex), and GAPDH as a loading control. * indicates non-specific band
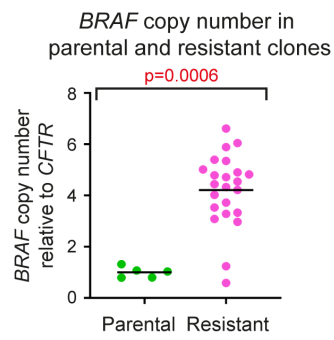
C. Quantification of EdU positive cells by flow cytometry in COLO205 cells treated with palbociclib and/or selumetinib at the indicated concentrations for 24 hours before addition of 10 µM EdU for 4 hours. Control cells were treated with DMSO only. Individual plots show EdU incorporation and DAPI staining of DNA for each sample as indicated, with rectangles to represent gates used to separate EdU positive and negative cells. Percent EdU positive cells are shown within the gates for each sample.

D. Quantification of EdU positive cells in **C**. n=4 (2 biological replicates each of parental COLO205 cells and single cell-derived clone 2), p values calculated by *t* test with Welch's correction.
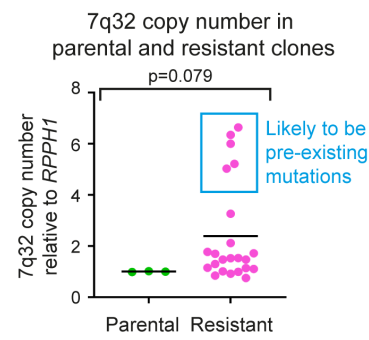
E. Effect of combined treatment with selumetinib and palbociclib on time taken for the emergence of resistant clones in parental COLO205 cell line. Cells were seeded in 6-well plates and allowed to settle for 24 hours, after which they were treated with 1 µM selumetinib in the absence or presence of 16 nM palbociclib. Media and drug were changed weekly, and the time taken for the appearance of first colony (≥50 cells) of proliferating cells in each well was recorded (in weeks). 12 independent replicates were performed under each condition, p values were calculated using the Mantel-Cox log-rank test on the principle that emergence of resistance can be represented as survival time of non-resistant cultures.

F. Effect of combined treatment with 1 µM selumetinib and 16 nm palbociclib in single cell derivatives of COLO205 cells determined as in **E.** Data for 4 different single cell derivatives of COLO205 are shown.

A *BRAF* copy number in parental and resistant clones

C 7q32 copy number in parental and resistant clones

B Parental

Unique resistant
Similar to parental

Unique resistant
Major differences to parental
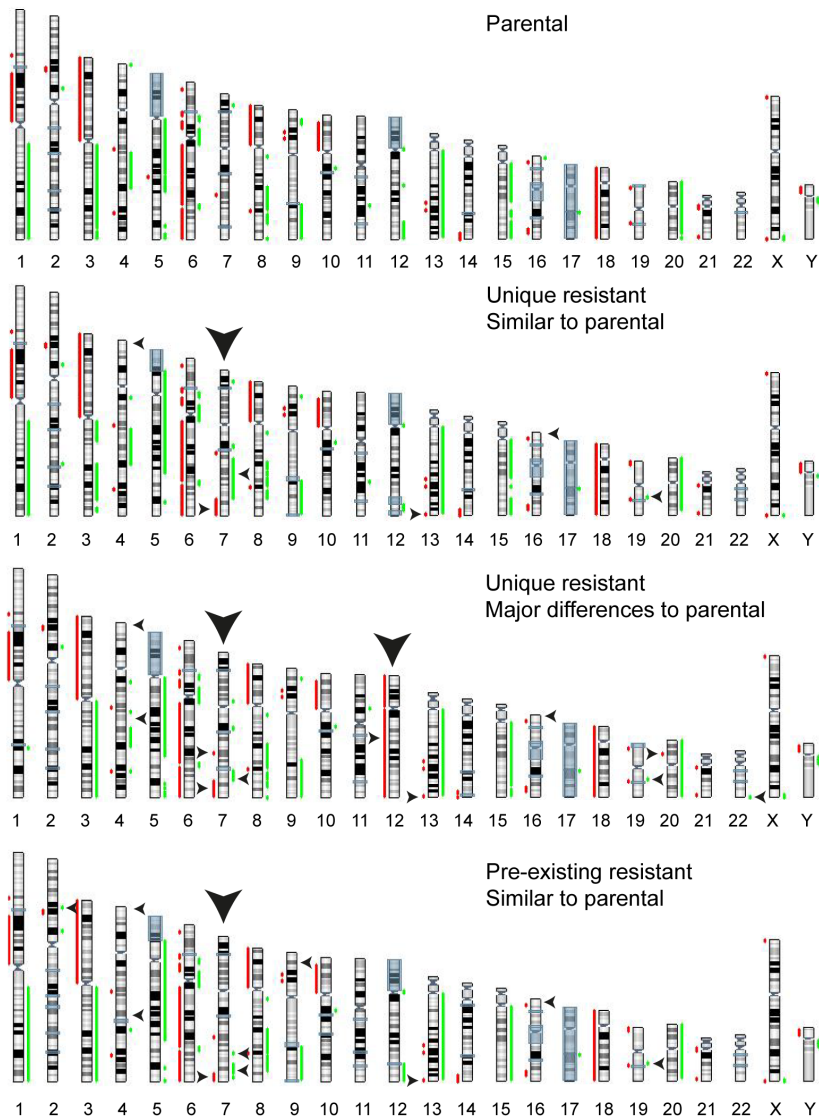
Pre-existing resistant
Similar to parental

Figure S1: Supplement to contributions of pre-existing and *de novo* gene amplifications to the emergence of selumetinib resistance in COLO205 cells

A. qPCR copy number analysis of *BRAF* (7q34) relative to *CFTR* (7q31.2) in parental and selumetinib-resistant lines derived as in Fig. **1A**. 21 of 23 selumetinib resistant cell lines show >3 fold amplification of *BRAF* relative *CFTR*. Each assay was performed in triplicate. p value was calculated by Mann-Whitney test, n=5 parental and 23 resistant.

B. Human chromosome ideograms showing CNVs across all chromosomes in parental COLO205 cells and 3 independently derived selumetinib resistant cell lines, profiled as in Figure **1C**. CNVs were called by BlueFuse, gains (right of chromosome) and losses (left of chromosomes) are represented in green and red respectively, loss of heterozygosity events are represented by grey boxes. Individual differences between resistant and parental cell lines were examined in primary data and excluded if copy number changes were small (<0.1), and therefore likely to be artefactual, could be explained by mis-calling of end-points of adjacent events. Differences between the lines that were not excluded are noted by small arrows, chromosomes showing differences across substantial regions are denoted by large arrows

C. qPCR copy number analysis of *RBM28* (located at 7q32) relative to *RPPH1* in parental and selumetinib-resistant lines derived as in Figure **1A**. Data for 3 replicates of parental COLO205 cells and 23 independently-derived selumetinib resistant cells lines are shown; 5 of 23 selumetinib resistant cell lines show amplification of *BRAF* relative *RPPH1*. Each assay was performed in triplicate. p value was calculated by Mann-Whitney test.
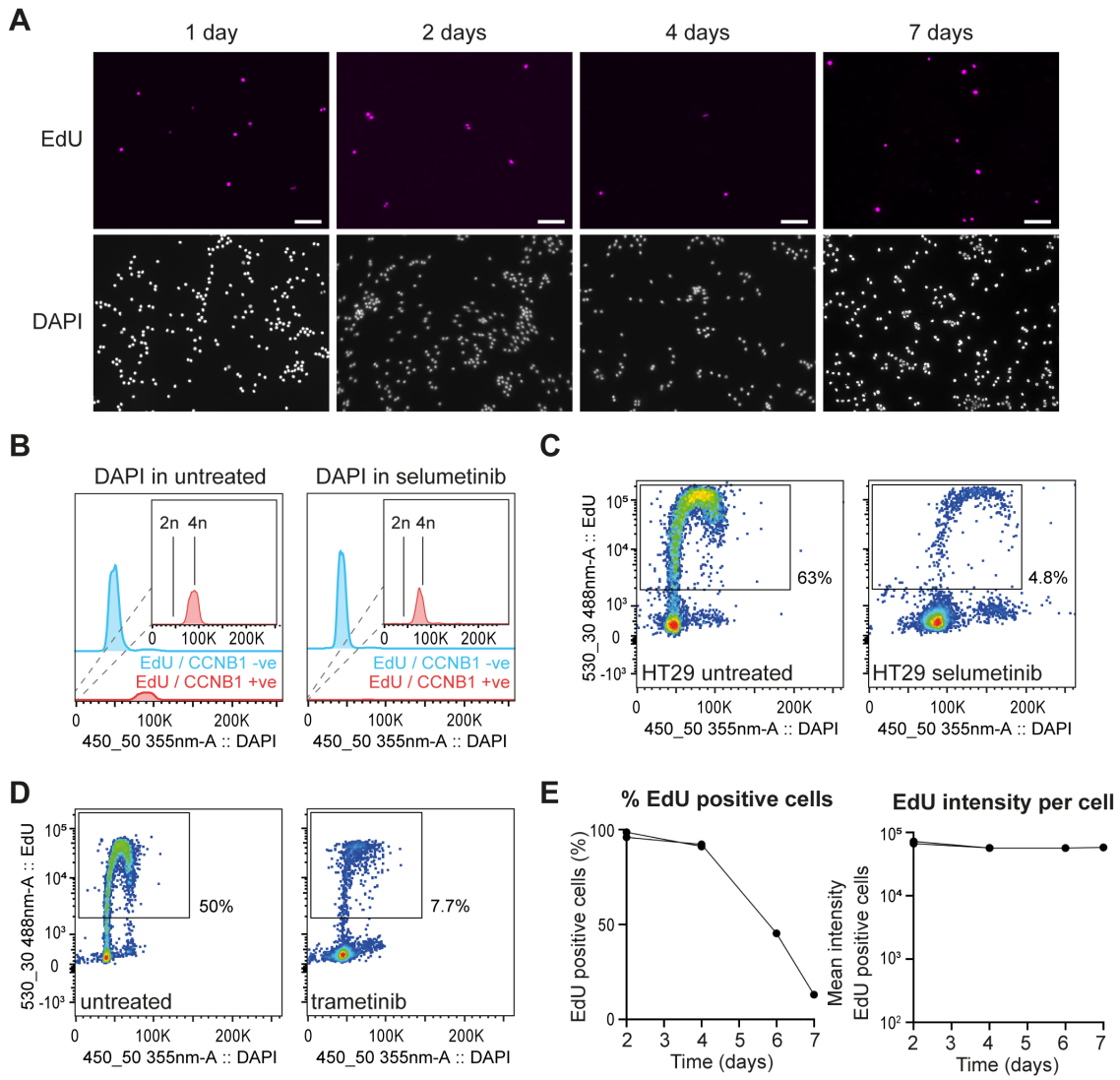
Figure S2: Supplement to replicating cells persist in long-term Selumetinib-treated cell cultures

A. EdU positive cells during prolonged selumetinib treatment. COLO205 cells were treated with 1 µM selumetinib for the indicated duration before addition of 10 µM EdU for 24 hours in the presence of selumetinib. EdU positive cells (pink) co-stained with DAPI (grey) from selumetinib treated cells are shown, scale bars represent 100 µm.

B. Fluorescence histograms of DAPI intensities for EdU / CCNB1 double negatives and double positives in untreated (left) and 1 µM selumetinib treated (right) COLO205 cells. Cells were treated with 1 µM selumetinib or DMSO only for 24 hours before addition of 10 µM EdU for 4 hours. EdU incorporation, CCNB1 and DAPI incorporation were determined by flow cytometry. Inset plots show DAPI intensities of EdU-CCNB1 double positives re-scaled to make rare EdU / CCNB1 double positive signals visible.

C. Quantification of EdU positive cells by flow cytometry in HT29 cells grown in the absence and presence of selumetinib. HT29 cells were treated with 1 µM selumetinib or DMSO only (untreated) for 24 hours before addition of 10µM EdU for 4 hours. EdU incorporation was detected by flow cytometry. Individual plots show EdU incorporation and DAPI staining of DNA for untreated (left) and selumetinib treated cells (right), with rectangles to indicate gates used to quantify EdU positive and negative cells.

D. Quantification of EdU positive cells by flow cytometry in COLO205 cells grown in the absence and presence of trametinib. Single-cell clone derivative (clone 1) of COL0205 cells were treated with 3 nM trametinib or DMSO only (untreated) for 24 hours before addition of 10 µM EdU for 24 hours in the presence of 3 nM trametinib. EdU incorporation was detected by flow cytometry. Individual plots show EdU incorporation and DAPI staining of DNA for untreated (left) and selumetinib treated cells (right), with rectangles to indicate gates used to quantify EdU positive and negative cells.

E. Quantification of EdU positive cells following a 24-hour EdU pulse during growth in the absence of selumetinib. COLO205 cells were treated with 2 µM EdU then washed with media and grown in culture for a period of 7 days. EdU incorporation was determined by flow cytometry on the indicated days, showing quantitation of EdU positive cells (left) and EdU intensity per cell (right), n=3. See Fig. 2E for more details.

C *Expresssion of genes highly responsive to MEK inhibition*

D *Expresssion of MEK signature genes*

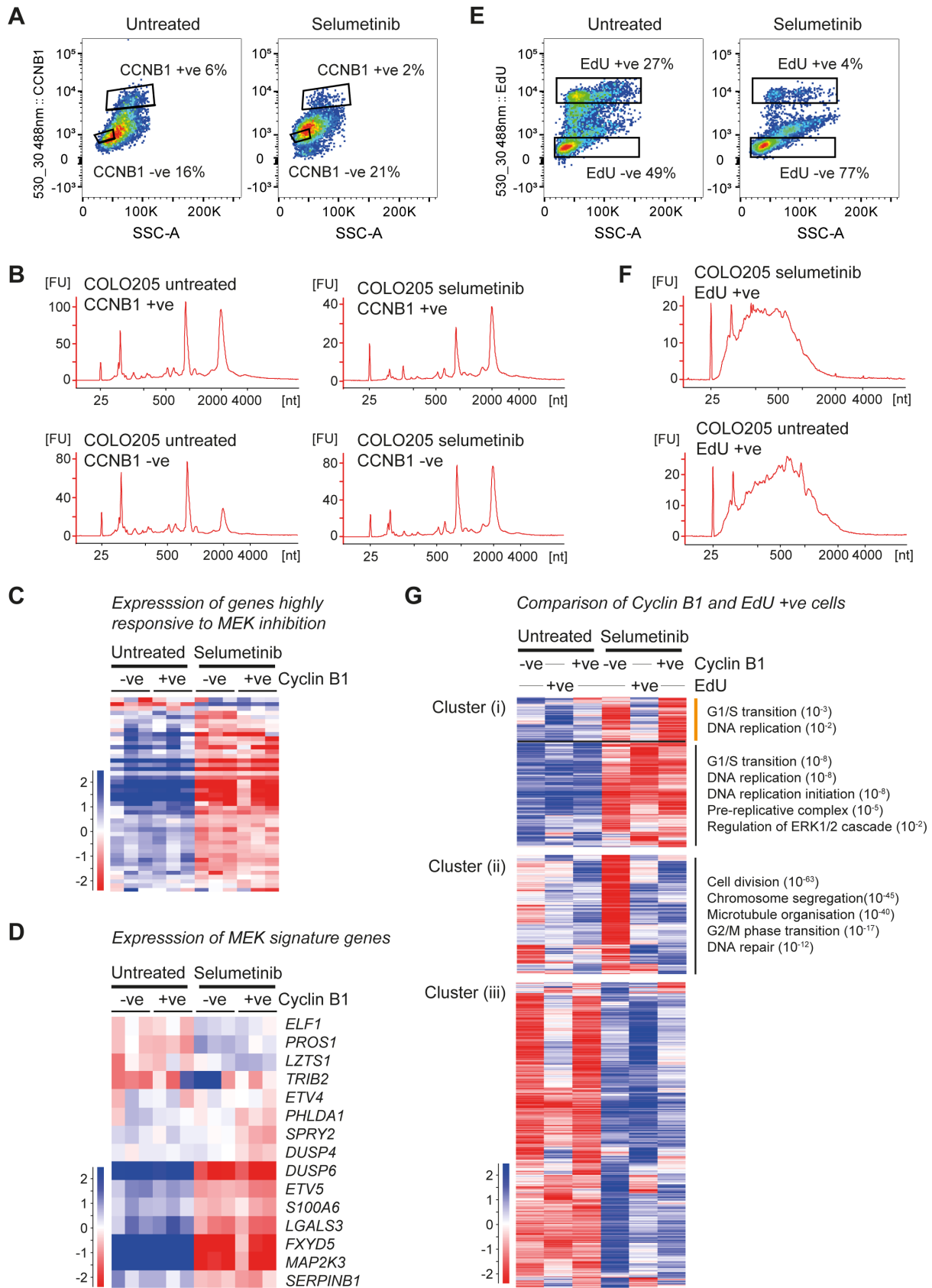**G** *Comparison of Cyclin B1 and EdU +ve cells*

Figure S3: Supplement to gene expression analysis of replicating cells

A. Flow cytometry density plot for COLO205 cells labelled with anti-CCNB1 primary antibody and donkey Alexa Fluor-488 conjugated secondary antibody and sorted using a BD FACSAria III sorter. Fluorescence thresholds for isolation of CCNB1 positive and negative cell fractions are shown. Gates were set based on a negative control staining without primary antibody, and the CCNB1 positive and negative sorting gates were set apart from each other to maximise sort purity.

B. Bioanalyzer profiles of total RNA isolated from CCNB1 positive and negative cells in untreated and 1 µM selumetinib treated cells sorted by flow cytometry using a BD FACSAria III sorter. 0.1-5 ng of total RNA was separated on total RNA pico chips on Agilent 2100 Bioanalyzer

C: Hierarchical clustering of gene set identified by Pratilas *et al.* (*47*) as significantly altered on MEK inhibition, showing relative expression in CCNB1 positive and negative fractions in the absence and presence of 1 µM selumetinib.

D. Hierarchical clustering of signature genes for MEK activity identified by Dry *et al.* (*49*) in CCNB1 positive and negative fractions in the absence and presence of 1 µM selumetinib.

E. Flow cytometry density plot for COLO205 cells stained for EdU and sorted using a BD FACSAria III sorter. Fluorescence thresholds for isolation of EdU positive and negative cell fractions are shown. Gates were set using the unstained negative control and the EdU positive and negative sorting gates were set apart from each other to maximise sort purity.

F. Bioanalyzer profiles of total RNA isolated from EdU positive cells in untreated and 1 µM selumetinib treated cells sorted by flow cytometry using a BD FACSAria III sorter. 0.1-5 ng of total RNA was separated on total RNA pico chips on Agilent 2100 Bioanalyzer

G. Hierarchical clustering analysis of the three clusters of genes significantly and substantially differentially expressed amongst CCNB1 positive and negative selumetinib treated cells and controls, as defined in Fig. 3C. CCNB1 data represents an average of 3 biological replicates, compared with EdU positive cells isolated from selumetinib treated and control cells in **E.** Gene expression data from EdU positive cells is similar to CCNB1 positive cells, except for the upper set of genes in cluster (i), highlighted in orange, that show transient upregulation in replicating cells. The full list of enriched GO categories (q<0.05) is presented in Table S3.
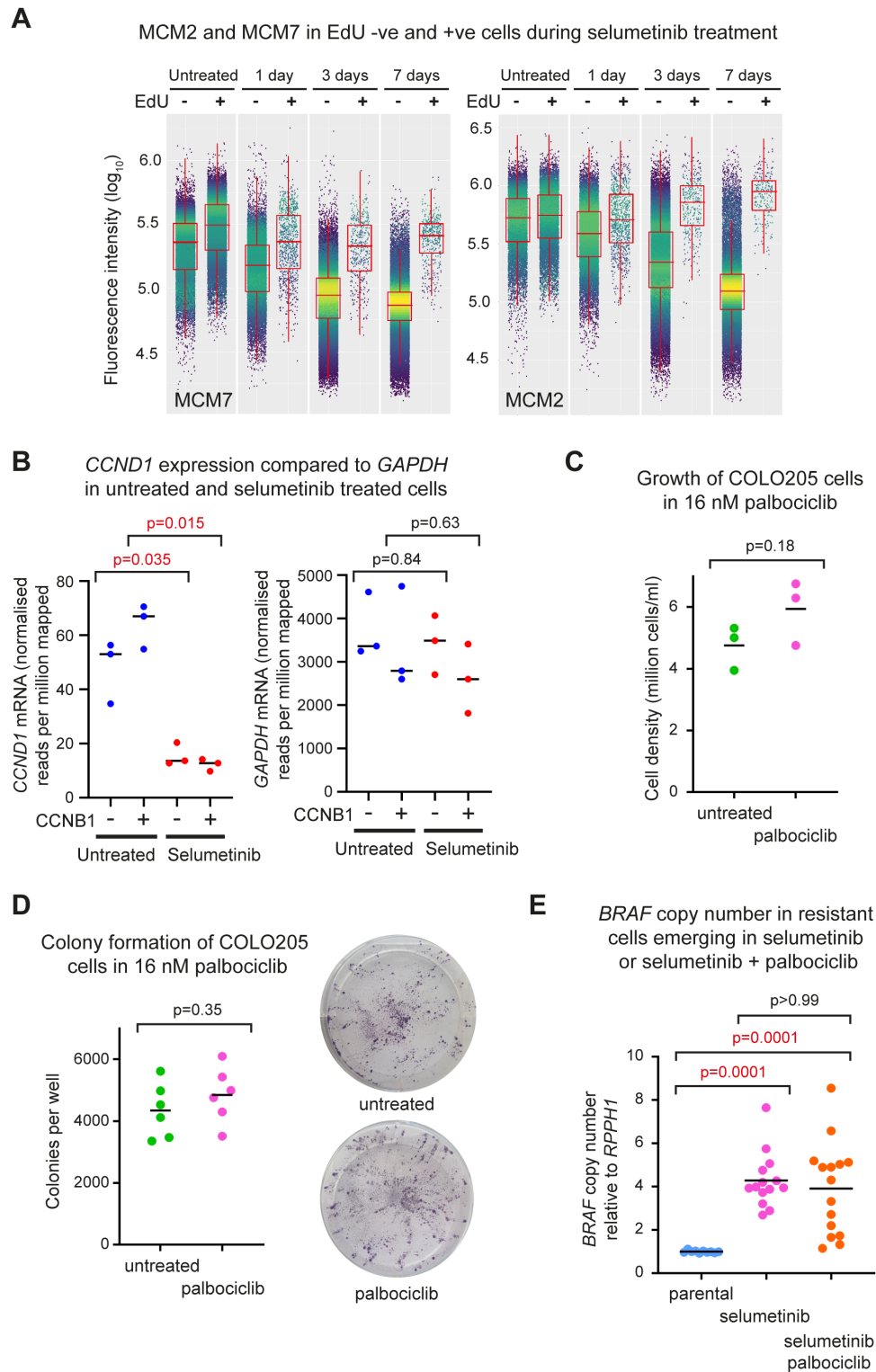
Figure S4: Supplement to suppressing DNA replication in selumetinib slows acquisition of resistance

A. Quantification of MCM2 and MCM7 in EdU negative and positive COLO205 cells treated with 1 µM selumetinib or DMSO only (untreated) for 1, 3 and 7 days before addition of 10 µM EdU for 4 hours. EdU incorporation and MCM2 and MCM7 levels were determined relative to unstained control cells by high content imaging analysis. Red boxes indicate median signal

intensity and inter-quartile range (IQR), whiskers indicate quartile range 1 – 1.5x IQR and quartile range 3 + 1.5x IQR.

B. Expression of *CCND1* (Cyclin D1) in untreated and selumetinib treated cells compared to *GAPDH* as an example housekeeping gene. Normalised read counts (reads per million mapped) from mRNA-seq of CCNB1 negative and positive cells show that *CCND1* expression is substantially repressed by selumetinib treatment, and is not upregulated in cells that have entered the cell cycle. n=3 biological replicates, p-values calculated by one-way ANOVA with a Brown-Forsythe and Welch correction.

C. Effect of single agent administration of palbociclib on cell growth in COLO205 cells. Cells were treated with 16 nM palbociclib or DMSO only and incubated for 7 days. Cells were harvested by trypsinisation and cell pellet resuspended in 1 mL culture media. Cells were counted using a Countess automated cell counter at the indicated times. p value calculated by t test, n=3 biological replicates.

D. Effect of single agent administration of palbociclib on colony formation in COLO205 cells. Cells were treated with 16 nM palbociclib or DMSO only and incubated for 24 hours. Following treatment, cells were harvested by trypsinisation and 100 cells seeded per well in 6-well plates in the absence or presence of 16 nM palbociclib and incubated for 21 days. Colonies were fixed and stained in 0.4% crystal violet in 50% methanol (representative images shown). p value calculated by t test, n=6 biological replicates per condition.

E: qPCR copy number analysis of *BRAF* relative to *RPPH1* in parental and selumetinib-resistant cell lines derived in selumetinib alone or selumetinib + palbociclib. COLO205 cells were treated with 1 µM selumetinib in the presence and absence of 16 nM palbociclib, and media and drug changed weekly until colonies of proliferating cells were observed. *BRAF* copy number relative to *RPPH1* in independent resistant clones was determined by qPCR analysis; DNA from log phase culture of parental COLO205 cells was used as control. Each sample was assayed in triplicate. p values were calculated by Kruskal-Wallis test (n=10 parental, 14 selumetinib, 15 selumetinib + palbociclib).